

**RECENT PALEOLIMNOLOGICAL HISTORY OF JACKSON LAKE, GRAND
TETON NATIONAL PARK, WYOMING (USA)**

THESIS

A thesis submitted in partial fulfillment of the
requirements for the degree of Master of Science in the
Arts and Sciences
at the University of Kentucky

By

Hillary Lynn-Anne Johnson

Lexington, Kentucky

Director: Dr. Michael McGlue, Professor of Geological Sciences

Lexington, Kentucky

2023

Copyright © Hillary Lynn-Anne Johnson 2023
[<https://orcid.org/0009-0008-2434-359X>]

ABSTRACT OF THESIS

RECENT PALEOLIMNOLOGICAL HISTORY OF JACKSON LAKE, GRAND TETON NATIONAL PARK, WYOMING (USA)

This study utilizes a recently acquired, high-resolution CHIRP seismic reflection dataset and a deepwater sediment core to analyze the recent stratigraphy of Jackson Lake (Wyoming, USA). The western shoreline of Jackson Lake is situated adjacent to the Teton fault, a down-to-the-east normal fault that produces the spectacular high topography of Grand Teton National Park. The sediments of Jackson Lake are underexplored and consequently, their value as indicators of hydroclimatic and tectonic changes is unknown. Here, the sedimentary fill of Jackson Lake is explored as a natural archive of environmental change, specifically in reference to the influence of human outlet engineering (dam installation) on the lake. This study developed new bathymetric, acoustic basement, isopach, and facies maps from seismic reflection profiles in order to illustrate the modern distribution of available accommodation, sedimentary depocenters, and features of the sublacustrine geomorphology. Major faults were mapped by identifying offset basement reflectors, and acoustic facies were characterized based on external geometry and internal characteristics of reflections. A major finding in the shallow seismic data were several prograding clinoforms; these features appear to reflect processes associated with lake level transgression due to installation of the dam, which resulted in the flooding of deltas. The northern axis of Jackson Lake displays high amplitude, parallel, semi-continuous lake floor reflections interpreted as flooded Snake River delta plain deposits, whereas low amplitude, continuous reflections in the basin center are interpreted to be hemipelagic lacustrine sediments. Evidence of glaciation is also present in the seismic dataset; mound-shaped acoustic geometries with limited penetration are interpreted as submerged drumlins or moraines. A short sediment core, dated with ^{210}Pb , ^{137}Cs , and ^{14}C , serves as ground truth for the shallowest seismic reflectors in the basin's primary depocenter, and provides initial insights into deepwater sedimentation rates. The geochronological data indicate that the core encompasses ~365 years from ~1654 to 2019 CE, and an acceleration in sediment accumulation may have resulted from dam installation. This research will help to guide future long sediment coring, which is needed in order to establish the long-term depositional history of the basin.

KEYWORDS: Dam, Grand Teton National Park, Lacustrine, Paleolimnology, Seismic Reflection, Radionuclide Dating

Hillary Lynn-Anne Johnson

04/02/2023

Date

RECENT PALEOLIMNOLOGICAL HISTORY OF JACKSON LAKE, GRAND
TETON NATIONAL PARK, WYOMING (USA)

By
Hillary Lynn-Anne Johnson

Dr. Michael M. McGlue

Director of Thesis

Dr. Michael M. McGlue

Director of Graduate Studies

04/02/2023

Date

DEDICATION

I dedicate my thesis work to my grandfather, James Green who was like a father to me.

He has been lost to Lewy Body dementia. One of my last goals for his lifetime was to finish my thesis while he was still cognitive so he could read it and be proud of me. He supported me throughout all my education and provided me with inspiration during my time of illness.

ACKNOWLEDGMENTS

My thesis would not be possible without the guidance of my committee. First, I would like to thank my Thesis Chair and Director of Graduate Studies, Dr. Michael McGlue, for assisting and mentoring me in all aspects of my thesis including work life balance, bouncing back from setbacks, discipline specific support, and recovery from major life events. In addition, I would like to thank Dr. Ryan Thigpen who helped build my foundational knowledge in structural geology and basin dynamics. Next, I wish to thank Dr. Kevin Yeager for contributing his expertise in geochemistry, which was tremendously helpful. Lastly, on the committee, I would like to thank Dr. Ed Woolery for his positivity throughout the process and supplemental support in understanding geophysics. Everyone brought expertise to the table that enabled me to grow academically and substantially improved the quality and integrity of my research.

In addition to the field specific and writing assistance above, I received equally important assistance from my medical team, Cindy Turner, and my boyfriend. I would like to thank my medical team of specialists, especially my neurologist, Megan Craft for helping me minimize my symptoms and providing much needed relief so I could continue my education. Next, I would like to thank Cindy Turner for helping me with executive disfunction and pushing through revisions. Finally, I would like to sincerely thank my boyfriend, Edward de Vries, who stuck by me during the worst period of my life and provided a source of stability during the diagnostic stage of my chronic illness and brain injury. Without them I would not have had the willpower to push through the pain to complete this thesis at all.

TABLE OF CONTENTS

ACKNOWLEDGMENTS	iii
LIST OF TABLES	vi
LIST OF FIGURES	vii
LIST OF ADDITIONAL FILES	viii
CHAPTER 1. INTRODUCTION	1
1.1 Introduction.....	1
CHAPTER 2. STUDY AREA	9
2.1 Geological Setting.....	9
2.2 Glacial History	11
2.3 Climate, Hydrology, and Limnology	12
CHAPTER 3. METHODS	17
3.1 Methods.....	17
3.2 Age-Depth Modeling	19
CHAPTER 4. RESULTS	21
4.1 Results.....	22
4.2 Bathymetry.....	22
4.3 Total Sediment Isopach.....	26
4.4 Shallow Acoustic Facies	28
4.5 Core Stratigraphy	35
4.6 Sediment Core Chronology.....	36

CHAPTER 5. DISCUSSION.....	38
5.1 Discussion.....	38
5.2 Evidence of Dam Installation from Seismic Facies.....	42
5.3 Evidence from Sediment Core 9B	47
CHAPTER 6. CONCLUSION.....	49
6.1 Conclusion	49
REFERENCES	53
VITA.....	64

LIST OF TABLES

Table 1	Ages and Uncertainties of Earthquakes	11
Table 2	Seismic Acquisition and Processing Parameters	17
Table 3	Radiocarbon ^{14}C Results	21
Table 4	Acoustic Facies Interpreted	27

LIST OF FIGURES

Figure 1 Study Area	2
Figure 2 Jackson Lake Dam 1906 VS Rebuilding 1916	4
Figure 3 Lake level Elevation Curve	5
Figure 4 Jackson Lake's Water Levels Against Different Hydrologic Proxies	14
Figure 5 Bathymetric Map with Key Profiles	23
Figure 6 Acoustic Basement Map	25
Figure 7 Isopach Map	27
Figure 8 Acoustic Facies Map	28
Figure 9 Acoustic Facies on Seismic Profiles	29
Figure 10 Topographic Map of Jackson Lake from the 1890s	31
Figure 11 Key Deepwater Seismic Profile	32
Figure 12 Clinoform Seismic Profiles	34
Figure 13 Core 9B Stratigraphy, Magnetic Susceptibility, and Age-depth Model	38
Figure 14 Drumlin Morphology	48

CHAPTER 1.

Introduction

Freshwater resources are continuously in demand due to their limited and uneven distribution, and this condition is likely to be amplified by climatic variability in the future (Thomson et al., 2005; Schlager and Heikkila, 2011; Acharya et al., 2012). The unevenness and scarcity of freshwater resources is relieved, in part, by human engineering of natural waterways. For example, dams regulate the water cycle by forming a reservoir. Dams are very important, because they help to prevent and control floods, influence sediment fluxes, and in some cases can provide opportunities for hydropower (Shotbolt et al., 2005). Impoundment of rivers can significantly transform the riverine geomorphology and ecology downstream of the dam. This occurs through: (a) reductions of peak flow and suspended sediment load, (b) alteration of water chemistry (e.g., temperature, oxygen concentration, etc.) and riparian vegetation, (c) promoting variability in nutrient fluxes due to soil erosion (i.e., channel bed degradation), and (d) spurring changes in benthic aquatic habitats (Williams and Wolman, 1984; Herschy, 2012). Creating a dam can not only change ecohydrology and patterns of sedimentation but can also influence the local people. Dams can constitute catastrophic flooding hazards if the structure fails, which could result in injuries or losses of life, property damage or losses, and various other economic impacts (Wieland, 2014). In the past century alone, a number of seismically induced dam fractures and failures have been recorded, including as examples the Shih-Kang Dam failure (Taiwan; 1999), the Ono Dam fracture (Japan; 1923), the Koyna Dam fracture (India; 1967), the Eklutna Dam fracture (Alaska, USA; 1964), and the Lower Van Norman Dam

fracture and partial failure (California, USA; 1994) (Calayir and Karaton, 2005; Pekau et al., 1995; U.S. Committee on Large Dams, 2000;).

In the western United States, dams are important to water resources due to some of the worst water scarcity issues in the country (Mekonnen and Arjen, 2016), coupled with high demand from agriculture and ranching activities (Holechek et al., 2020). Climate change can influence water resources in many ways, for example by shifting the timing of snowmelt runoff and increasing the variability of precipitation and evaporation (Hansen, 2017). In 1904, President Theodore Roosevelt authorized the Minidoka Project as part of the Reclamation Act of June 1902, in order to bring irrigation and power into areas that were categorized as uninhabitable sagebrush deserts, with the hopes of encouraging future settlement in the American west (Bureau of Reclamation, 2018; Ford, 2020). In 1906, the Minidoka Project created one of its first dams on Jackson Lake in north-western Wyoming, in order to provide a reliable source of water for settlers in southeastern Idaho and northwestern Wyoming, near the headwaters of the Snake River (Stene, 1993) (Figure 1).

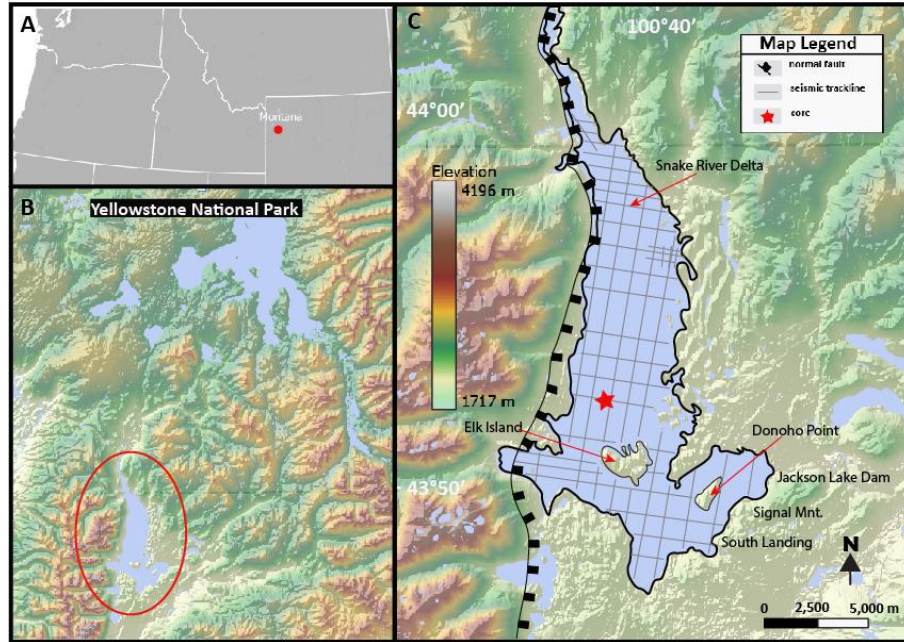


Figure 1: (A) A 1:20,000,000 country map depicting the surrounding western states, including Montana, Idaho, and Utah. (B) Regional elevation map showing the study site's proximity to Montana and Yellowstone National Park. The highest topography appears dark red and the lowest appears light green; water appears in blue (C) Study area in western Wyoming. Jackson Lake is outlined in black, and a red star indicates the location of the 9B sediment core station. The Teton fault is in black (teeth on the hanging wall side) along the western margin of Jackson Lake. Within the lake are the gray track lines along which the CHIRP seismic profiles were collected in 2018.

Jackson Lake was first converted into a reservoir using a temporary timber dam (Stene, 1993). This timber dam raised the surface of the lake 10 ft (~3 m), increasing the lake's capacity to 350,000 acre-feet (431,718,000 m³) (Stene, 1993). By 1910, the timber dam had rotted away and needed to be replaced. A new concrete gravity dam with embankment wings was erected by 1916 (Figure 2) (Stene, 1993). This new dam raised the water level to 847,000 acre-feet (1.04 x 10⁹ m³) and created what is known today as the Jackson Lake reservoir (Stene, 1993).

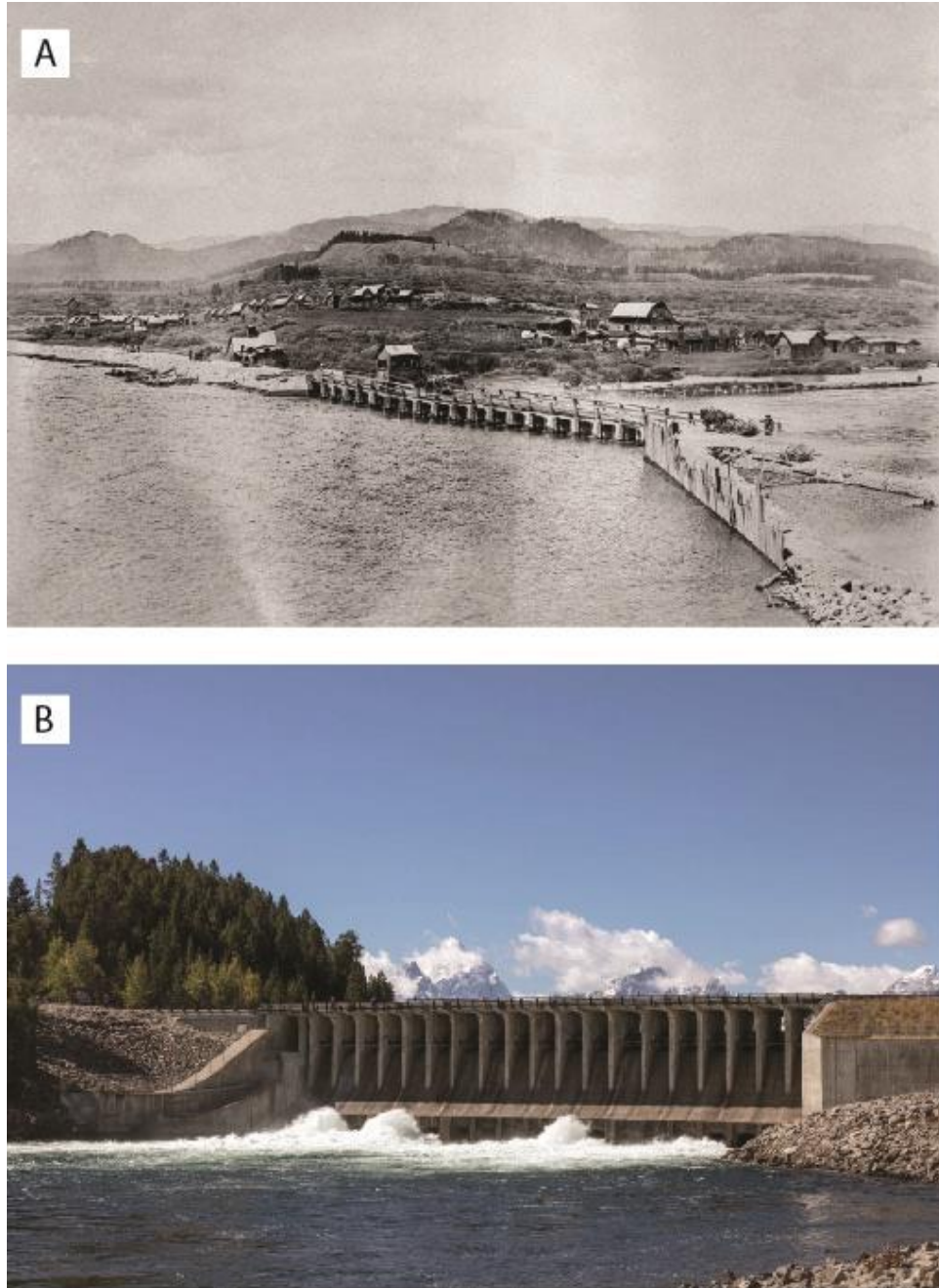


Figure 2: (A) Jackson Lake log-crib dam after its creation in 1906. Image credit: Jackson Hole Historical Society and Museum (<https://jacksonholehistory.org/jackson-lake-dam/>). (B) Jackson Lake concrete and earthen dam, rebuilt from 1911-1916, Image credit: Carol M. Highsmith, 1946 (accessed through the Library of Congress, <https://www.loc.gov/item/2017884802/>).

In 1990, the reservoir supported crops worth \$500M and that value has only grown towards the present day (Stene, 1993).

In certain circumstances, lake and reservoir sediments contain high-resolution records of catchment and atmospheric inputs such as radioactive particles, dissolved organic matter, microorganisms, acid, chemical compounds, and pollen through time and can be used as archives of ancient environments and geological processes (Shotbolt et al., 2005). Reservoirs typically have higher average sedimentation rates than natural lakes, with an average of ~20 mm/yr. (Shotbolt et al., 2005). The impoundment of Jackson Lake and the installation of a dam over the Snake River outlet provides the opportunity to study how this lake transitioned from a natural water body into a reservoir. Water level monitoring of Jackson Lake since 1908 by the U.S. Bureau of Reclamation has resulted in a high-resolution reservoir water level elevation dataset extending ~2017 (Figure 3).

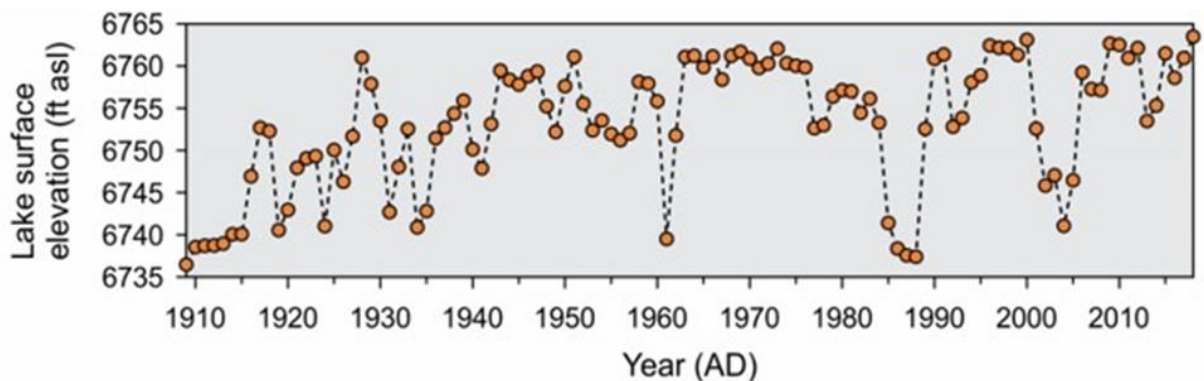


Figure 3: Mean annual lake level elevation data for Jackson Lake, 1908-2017 (Bureau of Reclamation, 2021). The lake shows a ~12 m transgression since dam installation. Major lowstands occurred in the 1930s, early 1960's, mid to late 1980s, and 2000s, due to construction to the dam or regional drought. See text for details.

In this study, those continuous water level elevation data are used to contextualize the influence of the dam installation on the limnogeology of Jackson Lake. The main question this thesis attempts to address is: How did transgression associated with the conversion of Jackson Lake into a reservoir influence sub-lacustrine geomorphological and

depositional processes? The completion of a permanent dam over the Snake River outlet (1916 Common Era, CE) is an important datum with respect to base level. This study uses both a well-dated sediment core and features mapped on high-resolution compressed high intensity radar pulse (CHIRP) seismic reflection profiles to address the main question of this study. The general approach was modeled after several other studies that used similar tools to evaluate the nature of sedimentation in reservoirs of the western USA. For example, Childs et al. (2003) conducted a bathymetric and geophysical survey on Englebright Lake, Yuba-Nevada Counties (California) to understand the nature of sedimentation following impoundment. That study is a useful partial analog, because Englebright Lake was converted into a reservoir in 1940, and it was influenced by a prograding delta, similar to the relationship between Jackson Lake and the Snake River (Childs et al., 2003). Snyder et al. (2006) expanded the work on Englebright Lake to reconstruct depositional processes and Englebright Lake's environmental history from its stratigraphy. That study used sediment core data and ^{137}Cs dating to assess sedimentation rates. Another study that was influential was conducted by Twichell et al. (2005) on Lake Mead in Nevada. In that case, Lake Mead was used as a natural laboratory to understand sediment transport and deposition in a regulated setting.

This study has important implications for our understanding of the history of Jackson Lake as a sedimentary system. Part of the environmental history of the past several centuries is linked to the climate change of the Little Ice Age (LIA), which originally was a term used to describe modest late Holocene mountain glacier advances. In the Greater Yellowstone Ecosystem (GYE), the LIA is believed to have extended from 1350–1850 CE (Mann et al., 2009; Rochner et al., 2021). Evidence for the LIA exists in many places

(especially in the Northern Hemisphere), but the timing was not globally synchronous. In the GYE, the LIA caused diatom blooms in lakes, major changes in terrestrial flora, a decrease in wildfire activity, and an increase in erosion under the cooler and wetter conditions (Bracht et al., 2008; Rochner et al., 2021). Ice core data from the Upper Fremont Glacier (northwestern Wyoming) shows periods of increased annual ice accumulation variability and a section of high-amplitude oscillations in $\delta^{18}\text{O}$ values that are linked to climate changes from the LIA (Naftz et al., 1996). Naftz et al. (1996) noted three distinct climate-related features in the ice core related to the LIA: (1) a shift to more negative $\delta^{18}\text{O}$ values, (2) an increase in small-scale variations in $\delta^{18}\text{O}$ signals, and (3) an abrupt shift from high-amplitude isotopic variations during the LIA to much lower amplitude isotopic variations characteristic of post-LIA ice. Thus, evidence for climate change exists in the areas near Jackson Lake, but it is yet unknown how this lake responded to these changes.

In the years following the LIA (~1850 CE to present day), the climate history of Wyoming has been influenced by its location in the middle latitudes and its proximity to the jet stream. Wyoming is susceptible to the impacts of winter storm systems, including heavy snows, high winds, and low wind chill temperatures (Frankson et al., 2022). Its interior position in North America far from oceanic moisture sources allows for a semi-arid climate. The state experiences large climatic variations, chiefly due to its physiographic diversity and altitudinal range. One major influence on the climate is the El Niño Southern Oscillation (ENSO). ENSO is a pressure pattern that switches back and forth between the Pacific and Indian oceans and is associated with changes in tropical Pacific Ocean temperatures (Yeh, 2009). La Niña is the oscillation that occurs when the contrast between warm western tropical Pacific and cool eastern tropical Pacific becomes

larger. La Niñas are linked to increased storms, dryer air in the east, and strong trade winds. El Niño is the oscillation that occurs when the central/eastern tropical Pacific is warm. This pattern causes storms, drying in the western Pacific and weak trade winds. Around Jackson Lake, historical observation data show that El Niño usually causes drier winters, whereas La Niña conditions results in higher winter snowfall. These patterns oscillate approximately every 3-7 years. Another climate pattern that may influence western Wyoming is the Pacific Decadal Oscillation (PDO). This is a recurring pattern of ocean-atmosphere climate variability centered over the mid-latitude Pacific Ocean basin. It includes two phases, a warm and cold phase (Mantua, 1999). During the warm (positive) phase, the surface water in the west Pacific Ocean cools, parts of the eastern Pacific Ocean warm, and sea level atmospheric pressures are below average over the North Pacific Ocean (Mantua, 1999). Conversely, the cold (negative) phase causes the surface water in the west Pacific Ocean to warm and parts of the ocean along the North American coast to cool, or above average sea level atmospheric pressures over the North Pacific Ocean (Mantua, 1999). The PDO primarily affects winter temperatures and precipitation in Wyoming.

In addition to the implications of Jackson Lake’s sediments for learning about climate history, there are also implications for understanding the earthquake history there. Major seismic activity has been absent over the past ~5,000 years on the Teton fault, and therefore earthquake hazards are deemed to be high in this region (Larsen et al., 2019; DuRoss et al., 2020; Thigpen et al., 2021). This study is a first step towards improving our understanding of Holocene and Pleistocene sediments in Jackson Lake, which could potentially be used to help fill the knowledge gap regarding the number and timing of earthquake events the region has experienced in the past, as has been demonstrated in a

number of other mountainous regions influenced by seismicity (Case et al., 2002; Moernaut et al., 2014; Moernaut et al., 2017; Strasser et al., 2013; Praet et al., 2020; Vandekerckhove et al., 2020).

CHAPTER 2.

Geological Setting

Jackson Lake (43.8928° N, 110.6749° W) is situated adjacent to the Teton Range, a tectonically complex location within the Rocky Mountains of the western USA. To the west, the lake is bounded by the Teton normal fault. To the south, Jackson Lake is surrounded by the Snake River Plain and Hoback Range. To the east, Jackson Lake is bordered by the Gros Ventre Range. To the north, the lake is bordered by the Yellowstone volcanic plateau (Behrendt et al., 1968; Thigpen et al., 2021). Uplift on the Teton fault likely initiated during the mid-Miocene, presumably through a combination of Yellowstone hotspot stress and Basin and Range extension (Behrendt et al., 1968; Brown et al., 2017; Thigpen et al., 2021). According to Behrendt et al. (1968), the Teton Range formed in two stages: (1) as a northwest-trending fold that deformed the Gros Ventre Range during the Late Cretaceous and early Tertiary, and (2) uplift of the southwest during the Cretaceous, late Paleocene, and Miocene associated with Basin and Range tectonism. Early estimates indicated that the Teton Range is ~60 km long and 15-25 km wide (Behrendt et al., 1968). According to new apatite fission track data collected from the footwall of the Teton fault coupled with flexural-kinematic modeling and length-displacement scaling relationships, the paleo-Teton fault and associated Teton Range may have been much longer, with the original length somewhere between 190-210 km (Thigpen et al., 2021). Brown et al. (2017) estimated that the minimum displacement on the Teton fault was at

least ~6 km, while newer research from Thigpen et al. (2021) supports a larger minimum fault displacement of ~11.4-12.6 km. At 190 km, the northern portion of this fault rests within the Yellowstone caldera, but the topographic signature of the feature is absent, likely having been “erased” via collapse into an evolving super caldera (Brown et al., 2017; Thigpen et al., 2021). The results of Brown et al. (2017) and Thigpen et al. (2021) suggest that the Teton fault could still be active, despite the absence of high topography north of Jackson Lake, posing a major seismic hazard to the region. If the fault is indeed longer, estimates for the potential magnitude of earthquakes must change, since the parameters for calculating magnitude include rupture length and slip rate (Anderson et al., 2016). This applies to the study area, because the Jackson Lake Seismic Network revealed that the Teton fault has not produced an earthquake greater than local Richter magnitude 3.0 between 1986-2002. This suggests that a progressive increase in strain energy may be accumulating along the fault (White et al., 2009; Thigpen et al., 2021). Teton fault quiescence and the influence of intraplate extension of the Yellowstone hotspot therefore pose major hazards in the “Intermountain Seismic Belt” (White et al., 2009). The Teton fault is thought to be capable of producing some of the largest earthquakes in this region, reaching a Moment Magnitude (M_w) of 7.2 (White et al., 2009). According to White et al. (2009), a trench at the Granite Canyon site provides information on the history of Teton fault rupture events (Table 1). Those trench data showed that paleoearthquakes took place at ~8.0 ka (~2.8 m of offset) and ~4.8 ka (1.3 m of offset). These data indicate that a higher slip rate characterized the Teton fault from 14-8ka, and that the fault slip rate varies through time (Smith et al., 1990; Byrd et al., 1995; White et al., 2009; Thigpen et al., 2021). Other studies of trench stratigraphy largely confirm the presence of those two major earthquakes

in the Holocene and perhaps a third at ~10 ka (e.g., Zellman et al., 2020; DuRoss et al., 2020). In contrast, lake sediments from nearby Jenny Lake suggest the possibility of even more earthquakes, though whether or not these events ruptured the entire length of the fault or affected a more localized area is still unknown (Larsen et al., 2019).

Table 1: Ages and uncertainties of earthquakes interpreted from trench sediments in the vicinity of Jackson Lake. These data suggest three earthquakes which occurred at ~10 ka, ~8 ka, and ~5 ka.

Paleoseismic Trench Studies		
Trench Location	Age (ka)	Author
Buffalo Bowl	9.9 ka (9.4–10.4 ka)	DuRoss et al., 2020
Buffalo Bowl	7.1 ka (5.5–8.8 ka)	DuRoss et al., 2020
Buffalo Bowl	4.6 ka (3.9–5.7 ka)	DuRoss et al., 2020
Granite Canyon	8.1 ka (7.8–8.3 ka)	Byrd, 1995
Granite Canyon	6.3 ka (4.8–7.8 ka)	Byrd, 1995
Leigh Lake	10.0 ka (9.7–10.4 ka)	Zellman et al., 2020
Leigh Lake	5.9 ka (4.8–7.1 ka)	Zellman et al., 2020
Leigh Lake	Possible 6.8 ka (6.5–7.1 ka)	Zellman et al., 2020
Steamboat Mountain	~4 ka	Zellman et al., 2018
Steamboat Mountain	~1.6 ka	Zellman et al., 2018

2.2 Glacial History

Jackson Lake is thought to have been created during the Pinedale stade ~15,000 YBP (Pierce and Good, 1992; Byrd, 1995; Larsen et al., 2016; Pierce et al., 2018). Grand Teton National Park (GTNP) was more directly shaped by the southern margin of the advancing Greater Yellowstone Glacial System (GYGS) during the Pinedale glaciation rather than the alpine valley glaciers exiting from the Teton Range (Pierce and Good, 1992). The Pinedale glaciation occurred in three stages that transformed the landscape previously shaped by an older glacial phase, known as Bull Lake, which occurred ~150 ka BP. The Pinedale glaciation streamlined and scoured the ground surface in Jackson Hole and deposited a complex series of moraines and outwash fans (Pierce and Good,

1992). Pinedale stage 1 scoured the Jackson Hole Basin (Pierce and Good, 1992; Byrd, 1995). Pinedale stages 2-3 included the advance and retreat of the Snake River ice lobe, which scoured the Jackson Lake basin during its recession (Pierce and Good, 1992; Byrd, 1995). Pierce and Good (1992) also noted that Jackson Lake was carved by confined subglacial meltwater jets, in evidence from eskers on the head of the South Landing outwash fan seen in Figure 1 (Pierce and Good, 1992).

2.3 *Climate, Hydrology, and Limnology*

Extant Jackson Lake covers 103 km² and is located ~2,064 m above mean sea level (amsl). Emplacement of Jackson Lake Dam forms a unique datum at 1916 CE, when lake levels transgressed to a new elevation of ~2,061 m amsl (*USGS 13010500 JACKSON LAKE NEAR MORAN, WY*, 2023). Jackson Lake's water level elevation is controlled by the dam, which is managed by the Bureau of Reclamation (*USGS 13010500 JACKSON LAKE NEAR MORAN, WY*, 2023). Apart from human control of the dam's spillway, the hydrology of Jackson Lake is strongly influenced by the Snake River, which enters the lake from the north. The Snake River exits Jackson Lake at its southeast margin, which is the location of the Jackson Lake Dam spillway. The Snake River may deliver sediments derived from the weathering of three different types of rocks into Jackson Lake: Quaternary rhyolite flows, Paleozoic/early Mesozoic sedimentary rocks, and Tertiary volcanic rocks from the Yellowstone Volcanic Plateau (Behrendt et al., 1968; Marston et al., 2005; Larsen et al., 2019). These sediments are largely coarse-grained due to slope failures along the Snake River valley (Marston et al., 2005). However, in our 2019 study we found the delta sediments consisted of high concentrations of mud and sand. The climate of Jackson Lake is strongly tied to its location in the middle latitudes, its position within the westerly wind

belt (jet stream), and the high topography of the surrounding landscape. Western Wyoming is susceptible to the impacts of severe winter storms, including heavy snow, high winds, and low temperatures due to its alpine setting and elevation range. The climate of the region falls in the Dsc Geiger-Köppen class (dry-summer subarctic) and is characterized by cold wet winters and dry summers, with at least three times as much precipitation in the wettest winter month than in the driest summer month. Winter moisture is carried by storm fronts that interact with the alpine topography and result in heavy snowfall in the Teton Range and ice-over of Jackson Lake (Kottek, 2006). These climate patterns are highlighted in Figure 4, which shows multiple trends through the years.

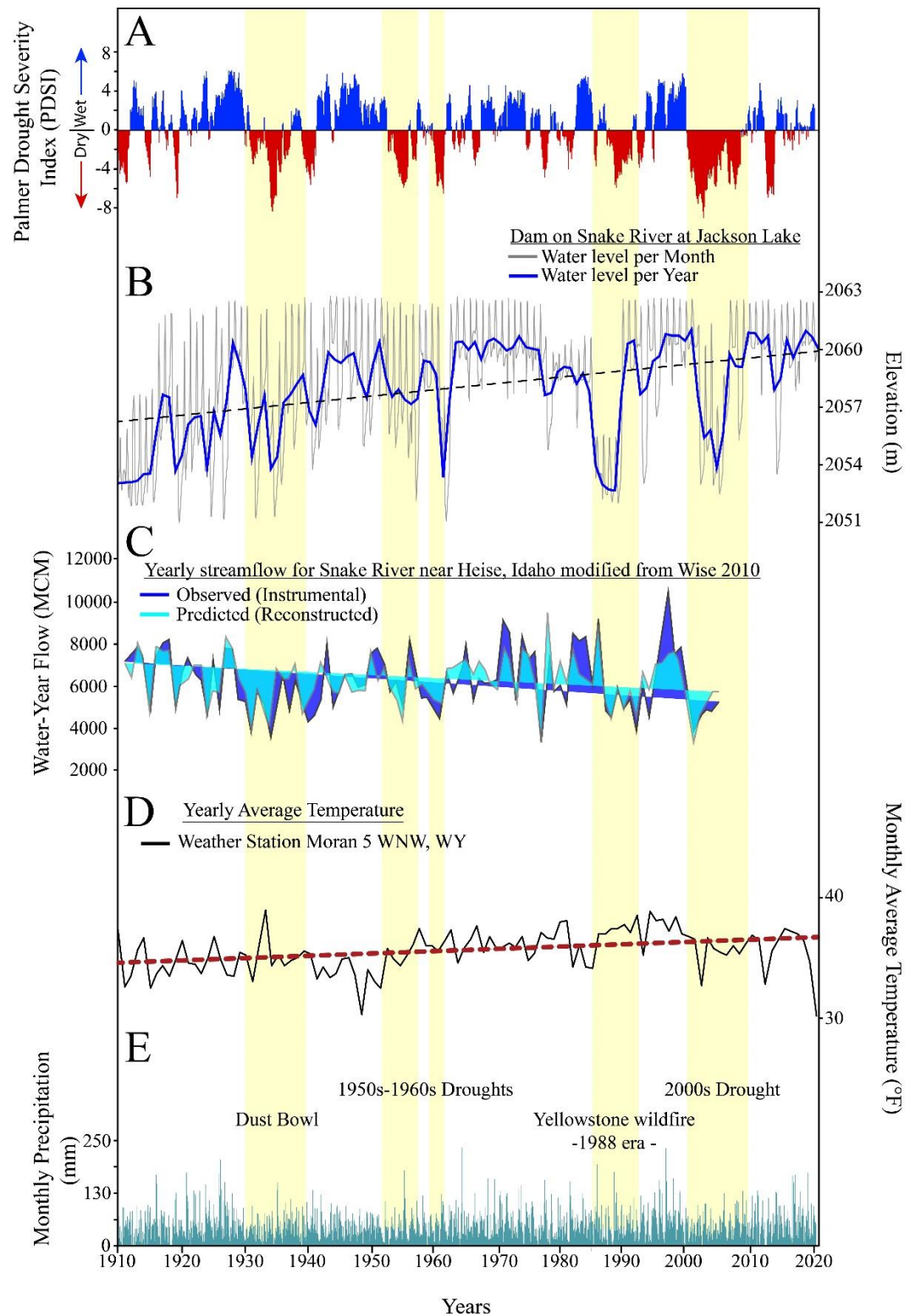


Figure 4: Dilworth et al. (2023) figure showing the trend between Jackson Lake's water levels against different hydroclimatic proxies from 1910-2022 CE. Pale-yellow bars

throughout the figure represent major drought intervals and regressions in Jackson Lake (Dilworth et al., 2023). (A) Palmer Drought Severity Index; (B) Monthly average water levels of Jackson Lake. Running average shown in dark blue line; (C) Annual Snake River flow near Heise, Idaho. Observed (dark blue) and predicted from tree-rings (light blue) are plotted for the period of interest; (D) Average annual temperatures (black line) with a long-term trend shown in red; (E) Monthly average precipitation (Dilworth et al. 2023).

Jackson Lake fluctuates around an average monthly temperature of 18° C in July and around 7° C in January (i.e., the coldest months where the lake is not frozen) (USGS 13010065 SNAKE RIVER AB JACKSON LAKE AT FLAGG RANCH WY, 2023).

Water levels in Jackson Lake appear to respond sensitively to climate change (Figure 3). For example, major droughts associated with the Dust Bowl in 1930–31, 1934, 1936, and 1939–40 were reflected in reduced water level elevations in Jackson Lake (Egan, 2005). The basin type and style of sedimentation is most likely controlled by its open hydrology; Jackson Lake is considered overfilled following the classification of Carroll and Bohacs (1999), meaning that fluvio-lacustrine facies associations and thickening of the stratal package toward major deltas are anticipated.

Very little other information has been published on the limnology of Jackson Lake. One study by Wurtsbaugh (2014) collected vertical profiles of temperature, oxygen, chlorophyll, and transparency to a maximum depth of ~59 m, which is a little more than half of the lake's maximum depth. The photic zone was situated at depths from ~11 to 16 m below the lake surface, suggesting high water clarity and light penetration (Wurtsbaugh, 2014). Wurtsbaugh (2014) noted that deep chlorophyll measurements supported the interpretation that the lake is oligotrophic. The oxygen profile increases with depth, but it is unknown if the lake floor is saturated with O₂ in the deepest parts of the lake. Wurtsbaugh (2014) suggested the possibility of seiche (internal waves)

modification of the thermal structure on a seasonal basis. Kilham et al. (1996) conducted a nutrient and productivity study using diatoms in the nearby Yellowstone lakes and Jackson Lake in GTNP that suggested Jackson Lake is mesotrophic. This mesotrophic state is supported by a diatom assemblage study done by Dilworth et al. (2023).

CHAPTER 3.

Methods

A geophysical survey was conducted on Jackson Lake in 2018, and > 100 km of compressed high-intensity radar pulse (CHIRP) seismic reflection profiles were collected. The survey parameters are summarized in Table 2. Native Edgetech .jsy files were digitally recorded in the field and subsequently converted into .seggy files for processing and interpretation. The .seggy files were loaded into Seisware 10.4 for analysis. Each line was processed using a bandpass filter set at 0.1-10.0 kHz to 0.2-8.0 kHz, and an Automatic Gain Control (Table 2). Several lines were also processed in HYPACK software, where time variant gains, bandpass filters, and top mutes were applied to improve the signal to noise ratio and clarify features in the subsurface.

Table 2: Seismic acquisition and processing parameters for the 2018 Jackson Lake CHIRP seismic survey.

Seismic Acquisition and Processing Parameters	
Acquisition system	Edgetech 3200 XS
Source and receiver	Edgetech SB-0512i CHIRP sub-bottom profiler
Source depth	0.5 m
Power	2000 W
Frequency Range	0.4-4.0 kHz (CHIRP pulse)
Pulse length	5 ms
Sampling rate	40 kHz
Navigation	Globalsat BU353S4 (USB GPS)
Processing	Bandpass filter, amplitude gain, (HYPACK) top mute
Vertical resolution	~12 cm

Basin-wide mapping of the lake floor (water-sediment interface) and acoustic basement (the level below which coherent seismic signals were lost) horizons was completed in SeisWare following standard principles of seismic stratigraphy (e.g., Scholz et al., 1993; Scholz et al., 2002). Major faults were identified where clear offsets

characterized the horizons; these faults were used to create polygons that were integrated into the grid and contour function of SeisWare. Important map products developed using SeisWare and its grid and contour functions included a bathymetric map and an acoustic basement map. A total sediment thickness (isopach) map was created by subtracting the water bottom (sediment-water interface) and acoustic basement grids in SeisWare. The bathymetry and acoustic basement grids were not the exact same extent given slightly different interpolations for each map, so the isopach map had to account for that variability, but the effect was negligible. All grids were contoured with a 20 ms two-way travel time (TWTT) contour interval in SeisWare. The SeisWare statistical technique used for smoothing the gridded data was minimum curvature; this was completed to produce more geologically realistic maps (Seisware International Inc., 2023).

Seismic facies analysis was conducted on each profile within a user-defined window that encompassed the upper ~10 ms TWTT of the sediment pile. This interval was chosen because only the uppermost facies were considered to have been influenced by outlet engineering. In assigning seismic facies types, the external geometry and internal acoustic characteristics of the shallow reflectors were evaluated (e.g., McGlue et al., 2006). All seismic profiles were assessed for the organization of reflectors (i.e., geometry or external form), as well as amplitude, continuity, and frequency (i.e., internal characteristics) to categorize facies. The shallow facies were tabulated, and the data were used to produce a lake-wide map, interpolating between lines using the grid coverage and extrapolating to the shoreline where necessary. These facies were made into maps using Adobe Illustrator for graphics processing.

Lastly, a sediment core (hereafter referred to as core 9B) was collected in July 2019 using an UWITECTM gravity corer. The sediment-water interface was captured and preserved in the field using hydrophilic floral foam. After collection, the core was sent to the Continental Scientific Drilling facility (CSD) for processing where it was split, imaged, scanned for physical properties on a GEOTEK multi-sensor and XYZ magnetic susceptibility (MS) loggers, and sub-sampled at 1-cm increments. Core sediments were described using standard techniques, identifying the variations in: 1) lithology and color, 2) bedding thickness and inclination, 3) sedimentary structures, and 4) disturbances caused by the coring process (Schnurrenberger et al., 2003).

3.1 Age-depth Modeling

Geochronological tools were used to quantify sediment accumulation rates in core 9B. The primary method used in this study was fallout radionuclide dating, following methods described in Yeager et al. (2004). Ages were produced at the Sedimentary, Environmental, Radiochemical Research Laboratory (SER₂L) using ¹³⁷Cs and ²¹⁰Pb, which were measured using gamma spectrometry and alpha spectrometry, respectively.

The ²¹⁰Pb activity concentrations were determined using alpha spectrometry. The alpha spectrometer used in SER₂L is a model 7404 Canberra integrated alpha spectrometer. The constant flux-constant sedimentation (CF-CS) model was used to produce rate information for core 9B following the equation of Appleby and Oldfield (1983):

$$[I(z)] = [I(0)]^{(-\alpha t)} \rightarrow \alpha = (\lambda/S)$$

where $[I(z)]$ and $[I(0)] = {}^{210}\text{Pb}_{\text{xs}}$ at depth z and the sediment-water interface, respectively; t = time (years); S = sediment accumulation rate ($\text{g cm}^2 \text{ yr}^{-1}$); α = the slope of the best fit line to the semi-log plot of ${}^{210}\text{Pb}_{\text{xs}}$ versus depth, and λ = decay constant (${}^{210}\text{Pb} = 0.031 \text{ yr.}$).

The ${}^{137}\text{Cs}$ ($E\gamma = 661 \text{ keV}$) activity concentrations were determined using gamma spectrometry on a Canberra High Purity Germanium (HPGe) well detector and multi-channel analyzers (DSA-1000). The ${}^{137}\text{Cs}$ sediment accumulation rates were determined using:

$$S = (D_{\text{pk}}/t)$$

Where S = sediment mass accumulation rate ($\text{g cm}^2 \text{ yr}^{-1}$), D_{pk} = the mass depth (g cm^{-2}) at which the 1963 peak in ${}^{137}\text{Cs}$ activity is found, and t = the time since 1963. ${}^{137}\text{Cs}$ typically exhibits an activity concentration peak in sediments corresponding to the year 1963, when the Partial Nuclear Test Ban Treaty was ratified (DeLaune and Buresh, 1978). Additionally, 1952 may be used since it was the first year that appreciable atmospheric fallout of ${}^{137}\text{Cs}$ was detected.

In addition to fallout radionuclide dating, five samples were delivered to the Beta Analytic Incorporated for radiocarbon (${}^{14}\text{C}$) dating using an accelerator mass spectrometer (Table 3). Four samples were fine-grained organic-rich sediments, and one sample was a charred twig. The organic-rich sediment samples were pretreated with dilute HCl to digest carbonate, and the woody material was pretreated with an acid/alkali/acid digestion, in order to remove contaminants that could influence age determinations. The top of the core was assumed to be 2019 CE (the year of core collection), and this assumption was supported by extrapolation of the average linear sedimentation rate derived from ${}^{137}\text{Cs}$ and

²¹⁰Pb. The radiocarbon dates required calibration for reservoir effects because of the large offset between ages between the wood and sediment organic matter collected from the same horizon.

Table 3: Radiocarbon (¹⁴C) results from the 9B core from Beta Analytics. Ages are reservoir-corrected using the paired wood/sediment ¹⁴C ages at 40 cm depth.

Depth (cm)	Material	¹⁴ C age (yrs)	¹⁴ C age uncertainty (yrs)	Reservoir corrected ¹⁴ C age (yrs)	δ ¹³ C (per mille)	Bacon-derived mean age (cal yr)	Bacon-derived 2-sigma age (cal yr)
40	Wood	90	30	90	-27.0	110	50-150
40	SOM	4310	30	90	-26.4	110	50-150
45	SOM	4480	30	260	-26.0	170	90-220
50	SOM	4430	30	210	-26.0	220	140-300
55	SOM	4680	30	460	-25.9	280	170-360

All ages were placed into the age modelling software Bacon for R to create a Bayesian statistics-based age-depth model (Blaauw and Christen, 2011). The Bacon parameters used for core 9B were: (a) depth minimum of 0 cm, (b) depth maximum of 57.5 cm, (c) an accumulation rate mean of 8 yr./cm, and (d) a section thickness of 1.5 cm. A slump was included to represent an event bed found in core 9B at 13-14 cm. In Bacon, the term slump is used for all features believed to represent instantaneous deposition without indicating a process of formation. Removing this event bed minimizes the margin of error by removing features that artificially thicken the strata without adding time, thus leading to overestimations in sedimentation rate (Strasser et al., 2013; Praet et al., 2016).

CHAPTER 4.

4 Results

4.1 Bathymetry

The bathymetry of Jackson Lake and select strike and dip bathymetric profiles are shown in Figure 5.

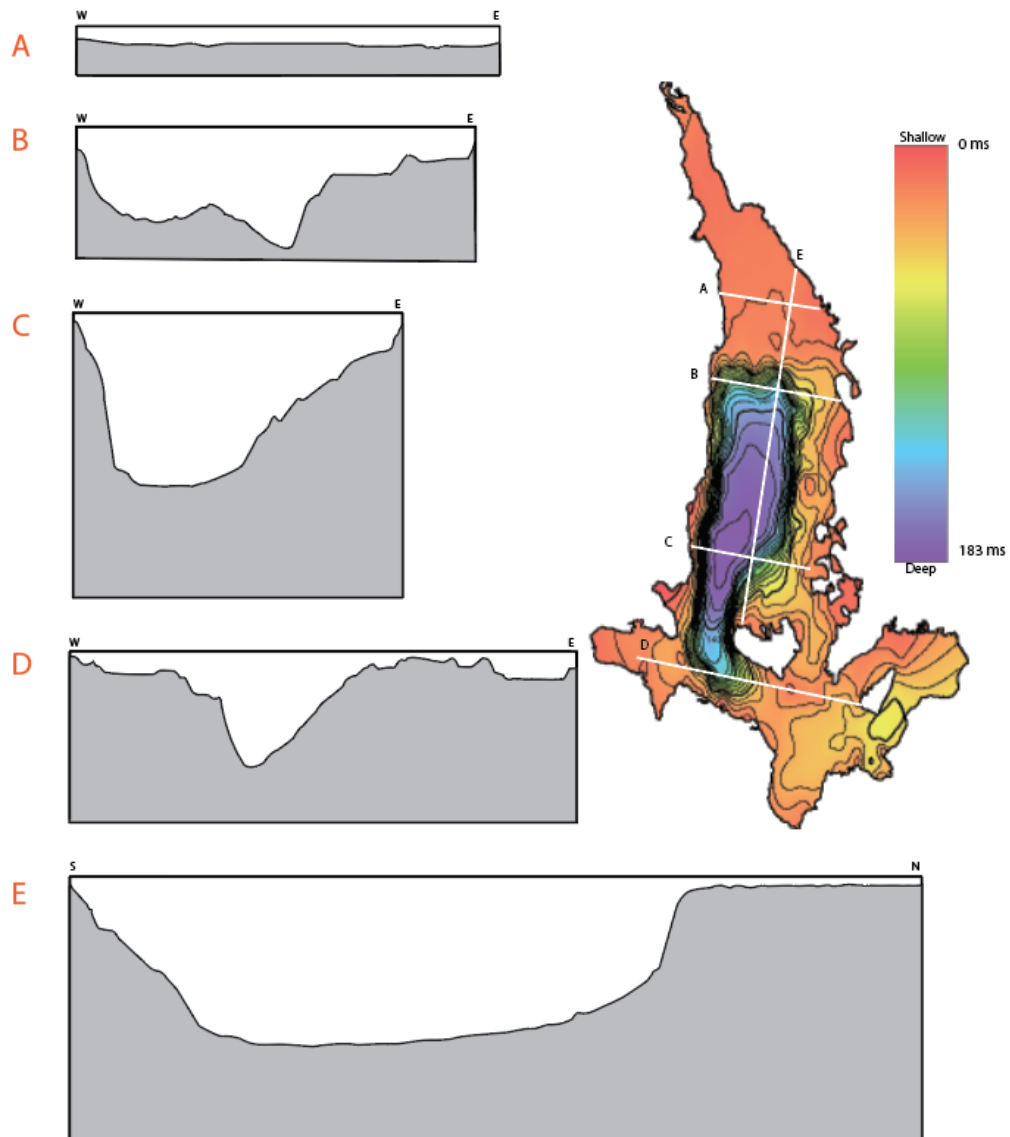


Figure 5: Bathymetric map for Jackson Lake, along with representative bathymetric profiles derived from mapping the water-sediment interface. Track line locations are labeled on map and orientation is labeled on each profile. Each profile is representative of

the zone of seismic characteristics that appear throughout the lake. Note that all profiles are vertically exaggerated. The bathymetric map highlights the presence of a major deepwater depocenter in the center of the lake, located adjacent to the high relief western lake margin.

The northern axis of Jackson Lake is shallow and relatively flat, with depths that range up to 13 ms TWTT. To the south, the basin deepens, with a slope positioned approximately parallel to Colter Canyon; the slope is relatively steep (approximate value?) and transitions into a deepwater depocenter that reaches a depth of ~190 ms TWTT in the center. This depocenter is confined by what I interpret to be several normal faults with opposing dips. On the east side of the basin, a down to the west normal fault creates a platform-like area on its footwall side, characterized by relatively shallow water depths. This fault is buried by sediments. The west side of the lake is defined by two down-to-the-east normal faults that exhibit minimal sediment drape. The larger of these two faults exhibits a steep slope of $\sim 12^\circ$. Only small, scattered pods of sediment are found on this steep and faulted margin. The two down-to-the-east faults measure ~6.5 and ~10.6 km long, whereas the opposing faults bounding the major depocenter that control the eastern margin platform measure about 4.5, 2.6, 2.2, and 2.2 km in length.

The central axis of the depocenter reaches a maximum depth of ~190 ms TWTT and in cross section has a “U-shaped” morphology. To the south, parallel to the northern shoreline of Elk Island, the lake floor appears to be influenced by a down-to-the-north-northwest fault, though it remains unclear if this a fault or a steep glacial scour surface. Additionally, Moran Bay is generally shallow (~?m), but is deeper than the average depth for the lake (~?m), reaching up to 60 ms TWTT deep. To the east, there are mound-like features that form positive relief on the lake floor that occur across a range of depths.

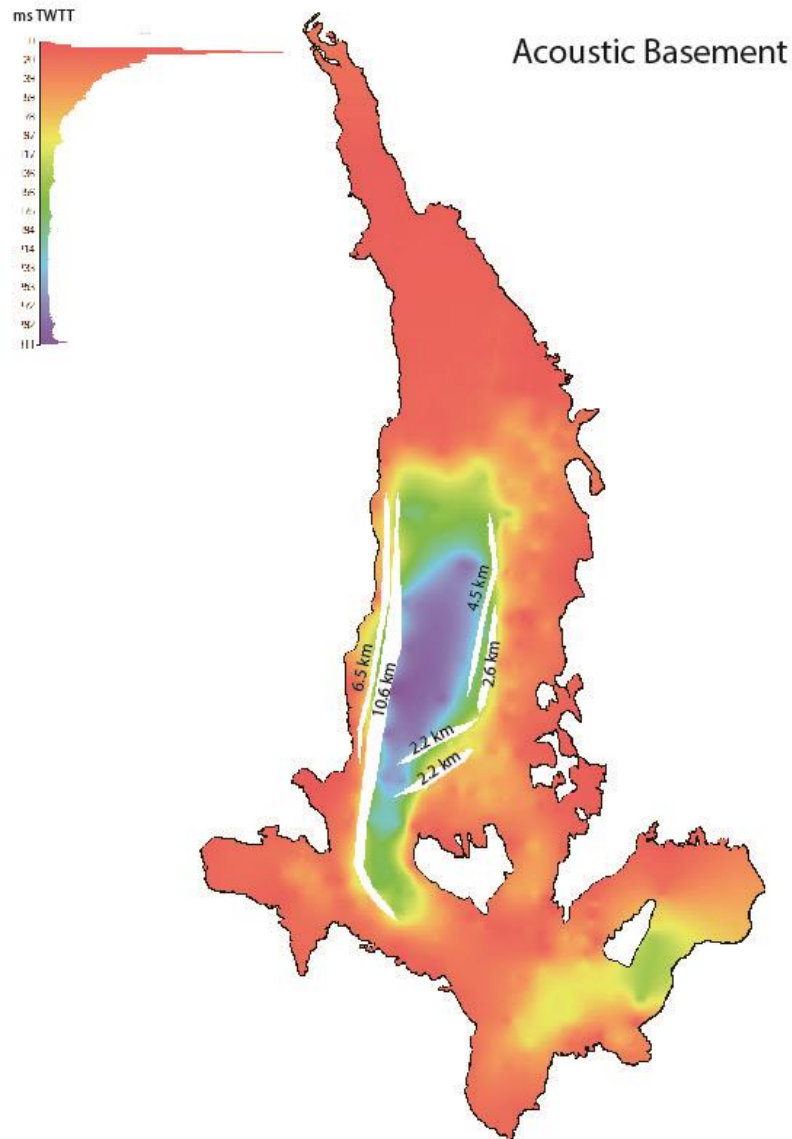


Figure 6: Acoustic basement map for Jackson Lake. White polygons are interpreted locations of normal faults.

The acoustic basement is very shallow in northern Jackson Lake and along the eastern flank of the basin. In most of these areas, little stratigraphy is discernable between the lake floor and acoustic basement reflections; in some cases, acoustic basement sits just above the first water bottom multiple. There are two areas of thick sediment accumulation in Jackson Lake that are readily discerned using the CHIRP seismic profiles. The lake's

major depocenter coincides with the area of the deepest water. This depocenter covers an area of $\sim 25 \text{ km}^2$, stretching from the area offshore of Colter Canyon in the north to southwest of Elk Island. The depocenter forms a tapered or boot-like morphology in plan view (Figure 6). The lake's stratigraphy to the north of the depocenter (Snake River delta) is often not easy to discern due to limited acoustic penetration, whereas extensive strata are well-imaged farther to the south in the depocenter. Acoustic basement in that area reaches a maximum of $\sim 311 \text{ ms TWTT}$, just north of Elk Island. A secondary, smaller depocenter is $\sim 7.6 \text{ km}^2$ and is situated south of Donoho Point, extending from the northeastern Spaulding Bay to the area close to the Jackson Lake Dam. The secondary depocenter reaches a maximum depth of 146 ms TWTT and averages 100 ms TWTT deep. The acoustic basement of Moran Bay reaches a maximum depth of 60 ms TWTT .

4.2 Total Sediment Isopach

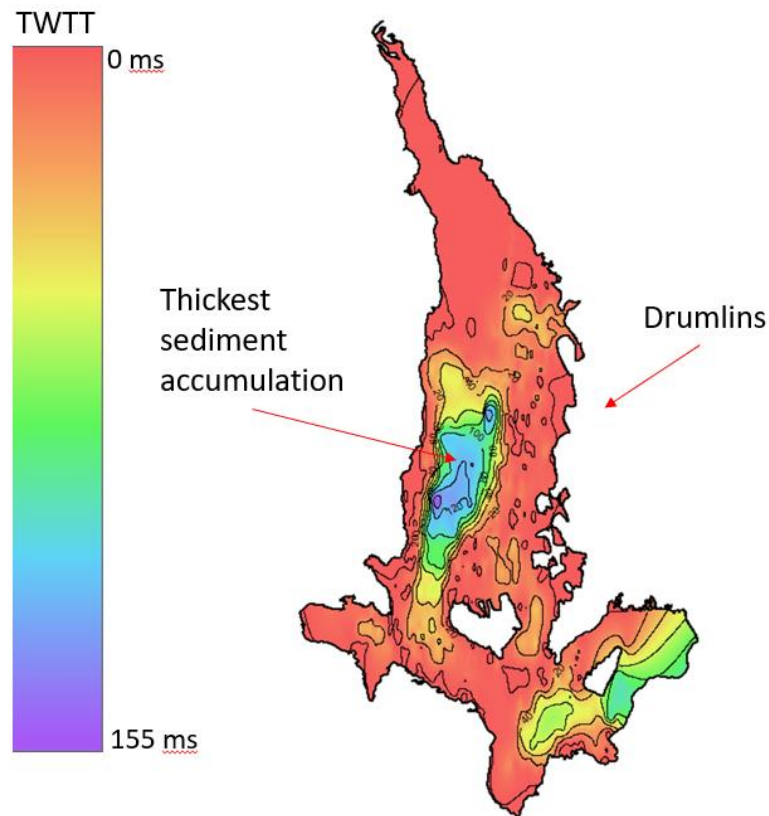


Figure 7: Isopach map showing sediment thicknesses throughout Jackson Lake with 20 ms TWTT contours. Lake sediments are thickest in the primary depocenter. See text for details.






The total sediment isopach map depicts the two key depocenters where accumulations of sediment are thickest, and this pattern is largely controlled by the variability in the depth of the acoustic basement. The main sediment package has a maximum thickness of 155 ms TWTT and an average thickness of 116 ms TWTT. The second sediment package measures ~99 ms TWTT thick in the center and it thins to ~58 ms TWTT on the edges. Along the eastern basin margin, numerous small, closed contours are present, which reflect the presence of mounds on the lake floor. The mounds in deeper water have acoustic drape, whereas the mounds in shallow water are more often exposed without draping low amplitude reflections. The largest mounds are located south of the

Arizona Creek inlet and close to Elk Island. Some of the smaller islands on the eastern side of the lake (Cow Island, Arizona Island, Indian Island, Sheffield Island and Moose Island) could represent subaerially exposed mounds as they appear to be similar in shape to the submerged mounds.

Shallow Acoustic Facies

Five shallow acoustic facies (AF) were identified on the Jackson Lake floor (Table 4).

Table 4: Jackson Lake floor acoustic facies interpreted within a 10 ms TWTT window .

Name	External Geometry	Internal Acoustic Characteristics	Interpretation
AF-1 	Sheet-like or tabular, occasional channel cuts, and fault offsets	High amplitude, parallel, semicontinuous lake floor return, discontinuous internal reflections	Submerged paleo-floodplain or paleo-lake margin
AF-2 	Basin fill	Low-moderate amplitude, parallel, continuous	Hemipelagic deposits
AF-3 	Clinoform	Low-moderate amplitude, sharply oblique to complex sigmoid-oblique, prograding reflections	Paleo-delta deposits
AF-4 	Mound	High amplitude, continuous – discontinuous lake floor return, minimal internal reflections	Submerged glacial till
AF-5 	Slope front	High amplitude, continuous minimal internal reflections with occasional drapes	Fault trace on possible bedrock

Sheet-like or Tabular Facies (AF-1)

Sheet-like or tabular facies consist of high-amplitude, low- to moderate frequency reflections that can be traced over long distances; this facies is especially concentrated in northern Jackson Lake (Figure 8 and 9). The reflections are most often parallel, semi-continuous to discontinuous. AF-1 exhibits a sheet-like, tabular external geometry with occasional shallow channel cuts or apparent faults with little offset. The basal surfaces of this facies follows the underlying topography.

AF-1 is interpreted as submerged paleo-delta plain, floodplain, or lake margin. Where sheet-like reflections are discontinuous, the best explanation is minor faulting or channel cuts associated with meanders on the drowned Snake River delta plain. A topographic map of Jackson Lake from the 1890s (Figure 10).

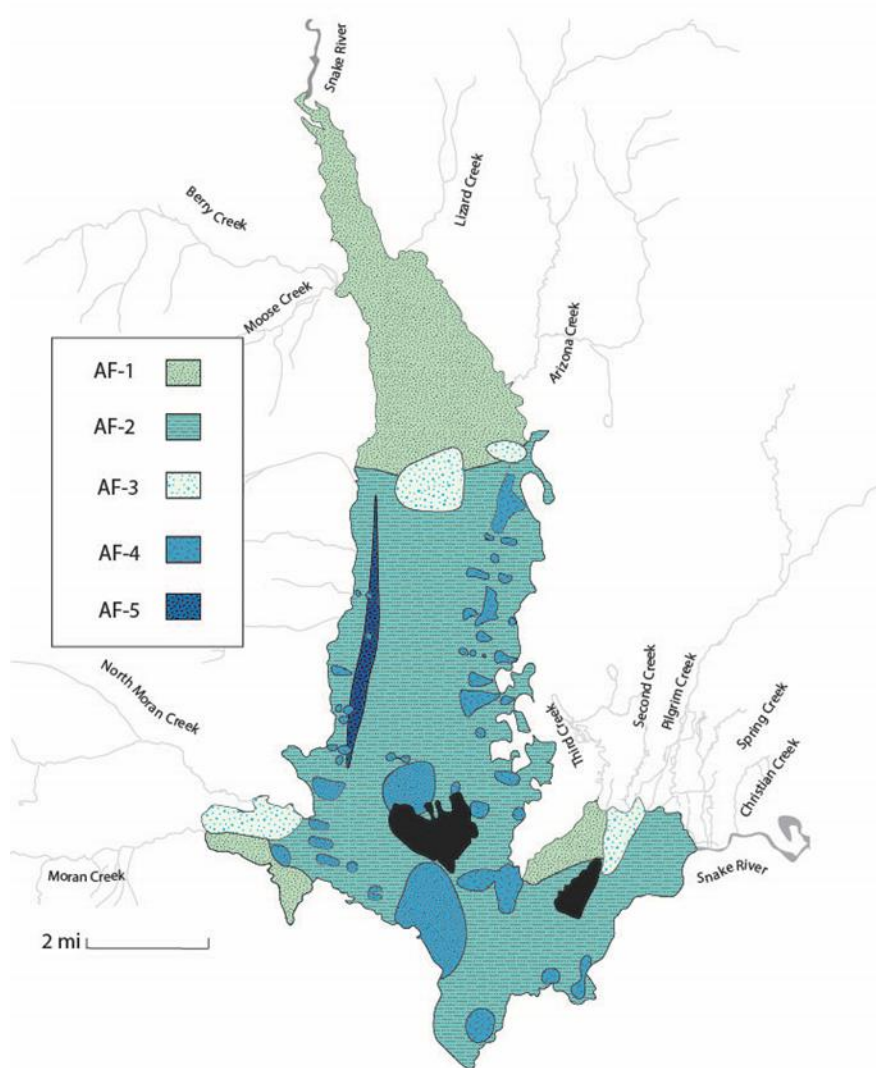


Figure 8: Acoustic facies map illustrating the location of different Jackson Lake floor deposits. Major inflowing rivers are illustrated in grey. AF-1 through AF-5 corresponds to Table 4. Islands appear in black.

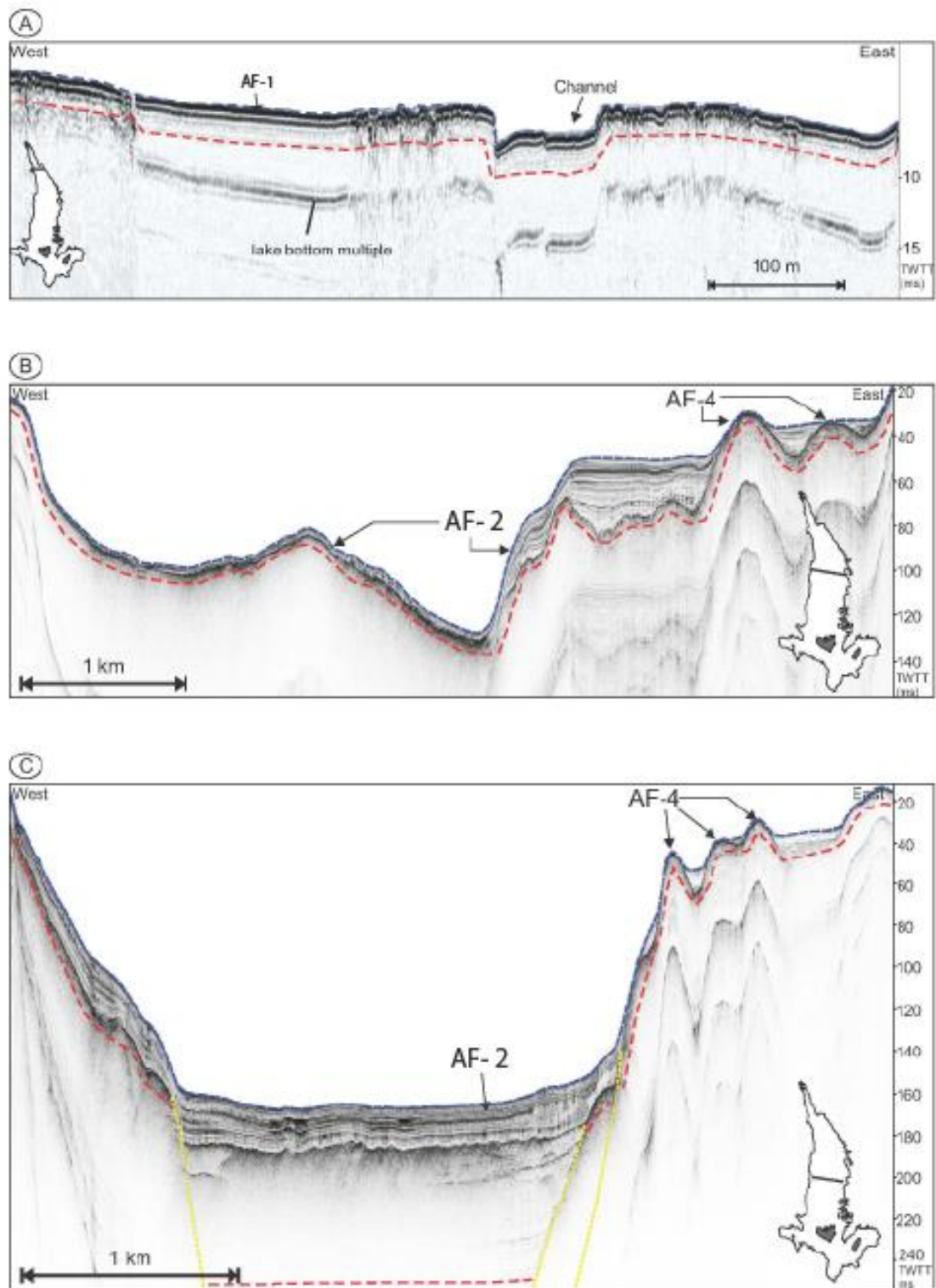


Figure 9: Acoustic facies examples on seismic profiles throughout the basin. The red dashed lines are the interpreted acoustic basement and yellow dashed lines are the interpreted faults. A) Shallow northern section of the lake, showcasing AF-1 (sheet/

UNITED STATES
DEPARTMENT OF THE INTERIOR
GEOLOGICAL SURVEY

WYOMING
(TETON COUNTY)
GRAND TETON QUADRANGLE

GRAND TETON NATIONAL PARK

JACKSON LAKE

SNAKE RIVER CANYON

GROS VENTRE MOUNTAINS

Mt. Moran
Mt. Myer
Mt. Wheeler
Teton Range

Jackson, Idaho
Teton, Wyo.

Scale: 0 to 10 Miles

U.S. Geological Survey

Topographic Map of Grand Teton National Park, Wyoming

Published by the U.S. Government Printing Office, Washington, D.C.

For sale by the U.S. Geological Survey, Federal Center, Denver, Colorado or Washington, D.C.

A folder describing topographic maps and symbols is available on request.

Figure 10: Topographic map of Jackson Lake area from the 1890s, illustrating the lake prior to installation of the dam at the Snake River outlet. Note the meandering channel of the Snake River north of the lake; today, this area is flooded when the lake is at highstand.

Basin-Fill Facies (AF-2)

AF-2 consists of low to moderate amplitude and moderate-frequency reflections (Figures 8, 9, and 11). Reflections in AF-2 are laterally continuous and extend many km within the depocenter, except where interrupted by divergent, chaotic reflectors. The external form of AF-2 is typically sheet-like, either draping underlying reflectors or filling available accommodation as symmetric basin fill or lenses (Figure 11). AF-2 consists of two different reflection characterizations. The parallel basin fill reflections are interpreted as hemipelagic deposits. Hemipelagic sedimentation is dominated by gravitational settling of suspended siliciclastic and biogenic sediments. The other reflection characterizations are the divergent or chaotic reflectors associated with mass wasting from the steep margins. These features appear as low amplitude with divergent or chaotic reflections that are organized as wedges or lenses adjacent to faults or steep slopes.

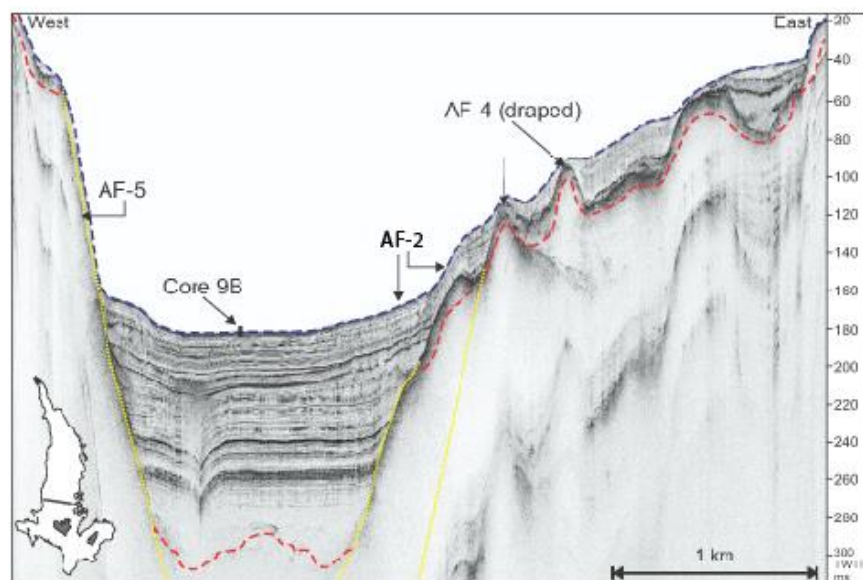


Figure 11: A key seismic profile collected in the deepwater depocenter located in the middle of Jackson Lake showcasing the location of the sediment core 9B relative to the acoustic facies. The core was collected from AF-2 (basin-fill) and is bordered by AF-5 (slope) and AF-4 (mound) facies. Again, the red dashed lines are the interpreted acoustic basement and yellow dashed lines are the interpreted faults. Seismic profile locations are shown as black lines on the map in the lower left corner and islands appear in dark grey.

Climoform Facies (AF-3)

AF-3 consists of low-high amplitude, discontinuous reflections arranged in packages of sharply oblique or complex sigmoid-oblique clinoforms (Figures 8, 12). In the oblique clinoforms, the basal surface underlying AF-3 is planar and marked by downlap of dipping foreset reflections. The upper bounding surface in the oblique clinoforms is marked by toplap terminations of foreset reflections. In complex sigmoid-oblique clinoforms, foresets grade into topset reflections, suggesting a component of aggradation during deposition. The AF-3 body aligned with the Snake River is 12 ms TWTT thick, AF-3 at Arizona Creek/Bailey Creek is ~5.8 ms TWTT thick, AF-3 at Second/Pilgrim Creek is ~9.5 ms TWTT thick, and AF-3 at Moran Creek is ~10.7 ms TWTT thick (locations in Figure 12). AF-3 is interpreted as paleo-delta deposits. The paleo-deltas are interpreted to be associated with base level changes in Jackson Lake that influenced the location of the mouths of different rivers, namely the Snake River, Arizona Creek/Bailey Creek, North Moran Creek/Moran Creek, and Pilgrim Creek/Second Creek/Third Creek (Figure 12). These clinoforms are helpful for base level quantification; the outermost topset to foreset roll-over point marks the paleo-lake level; in all cases, the rollover for clinoforms in Jackson Lake occur ~11-12 m below present lake level.

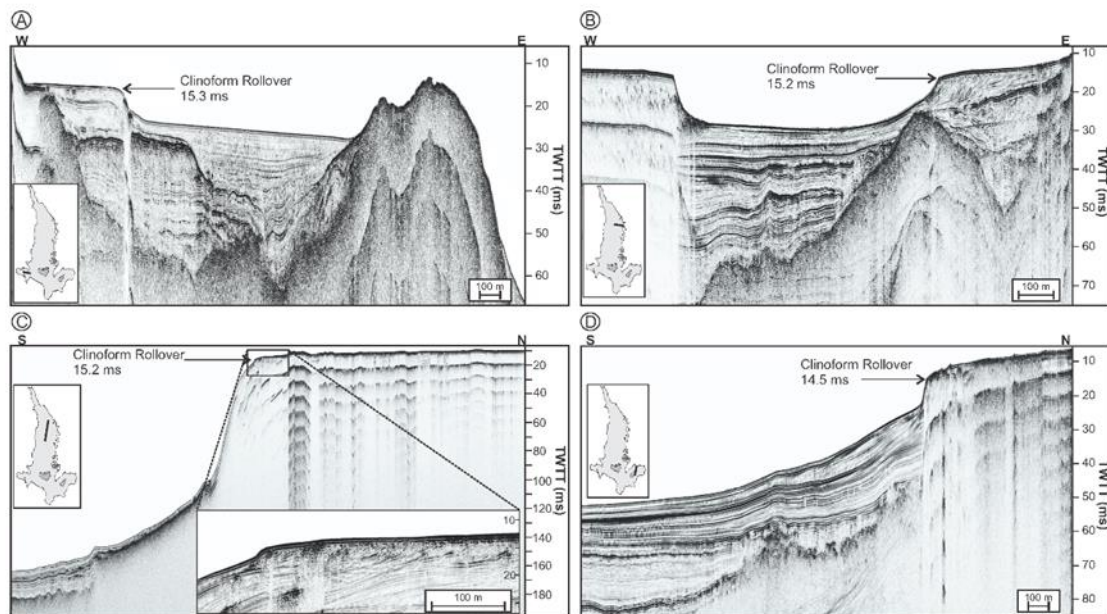


Figure 12: Seismic profiles capturing distinct clinoform examples from various locations within Jackson Lake, as depicted on the accompanying map to the left. Each profile exhibits a characteristic clinoform rollover. A) *Moran Bay - North Moran Creek/Moran Creek*: This profile illustrates clinoform steps observed in Moran Bay near the confluence of North Moran Creek and Moran Creek. B) *Arizona Creek/Bailey Creek*: This profile showcases the clinoforms located near Arizona Creek and Bailey Creek. C) *Snake River*: This profile displays the clinoforms associated with the Snake River. D) *Second/Pilgrim Creek*: This profile captures the clinoforms linked to Second Creek and Pilgrim Creek.

Mound Facies (AF-4)

AF-4 consists of high-amplitude, continuous to discontinuous lake floor reflectors with minimal sub-bottom penetration or internal reflectivity (Figures 8, 9). The external geometry of these deposits are prominent mound-shaped features that produce positive lake floor relief. The scale of these mounds' ranges from ~130 m to more than 2,000 m in diameter. The AF-4 mounds are interpreted as submerged accumulations of glacial till. Given their concentration along the eastern side of the basin, these features appear to be the offshore continuation of a set of drumlins that form a field onshore (Pierce et al., 2018).

The high-amplitude reflections with minimal internal properties are interpreted to result from dense, poorly sorted, mostly coarse-grained sediments.

Slope-Front Facies (AF-5)

The distribution of AF-5 is limited to areas associated with the submerged trace of what is interpreted to be the Teton fault; it is isolated on the western side of the basin, along the margin of the primary depocenter. AF-5 is defined by a sharp reflection with numerous diffractions along a very steep slope (Figure 8). Internal reflectivity and sub-bottom penetration are both minimal in AF-5. Several small pods and lenses of low amplitude reflections (AF-2) of varying thicknesses are found near the crest of AF-5. The high amplitude character and numerous shallow diffractions are interpreted as bedrock.

The northern end of Jackson Lake is chiefly made up of AF-1, which extends from the Snake River inlet south to the slope transition into the deepwater depocenter offshore from Colter Canyon. In the basin's northern axis, AF-1 is replaced by AF-3 clinoforms in two locations. There is a clinoform (AF-3) that progrades to the southwest oriented offshore of Arizona Creek – Bailey Creek. Adjacent to the Arizona Creek clinoform, but in the center of the lake, is the Snake River clinoform that progrades to the south. The slope it creates is 5.4° and prone to failure. Two additional paleo-delta clinoforms exist in the southern portion of the lake, one clinoform in Moran Bay that progrades to the east and another on the east side of the lake north of Donoho Point at Second and Pilgrim Creeks. AF-2 (basin fill) is the dominant facies covering much of the depocenter; it is very common in water depths that exceed 80 ms TWTT. Occurrences of AF-4 (mounds) cluster to form positive relief features along the eastern platform of the lake and then wrap around Elk Island, increasing in size and sediment volume. Moving south from Elk Island, the mounds

decrease in size and coalesce on the southwestern side of the lake in Moran Bay. AF-5 is localized on the western margin of the lake, coincident with the down to the east normal fault that bounds the main depocenter interpreted to be the trace of the Teton fault, or alternatively another large normal fault synthetic to the Teton fault. AF-5 extends from Waterfalls Canyon to the north side of Moran Bay. The southern end of the lake is dominated by AF-1 and AF-2, except where interrupted by mounds or paleo-deltas.

Core Stratigraphy

Four different lithofacies are present in core 9B: (1) diatomaceous silt, (2) laminated silty ooze, (3) inter-laminated silty organic-rich ooze, and (4) structureless silty ooze. Note that much of the core 9B sediments contain diatoms, which are a type of ubiquitous siliceous algae found in freshwaters globally. The sediments also contain siliciclastic detritus, which has an influence on the magnetic susceptibility curve and was used to detect the presence of ferromagnetic grains that are delivered to the lake from sources in the watershed. The magnetic susceptibility (MS) generally decreases from the base to the top of the core (Figure 13). The basal ~18 cm of core 9B consists of tan-colored diatomaceous silt with occasional planar continuous laminae and planar discontinuous and truncated laminae. The contact with the overlying unit is sharp and especially clear in the x-radiograph (Figure 13). This marks a transition into darker tan, laminated silty ooze with planar parallel continuous lamina and two wavy laminae. The laminated silty ooze lithofacies is only ~4 cm thick and is considered a transitional facies. Overlying the laminated silty ooze is a ~30 cm package of inter-laminated black, organic-rich ooze and tan silty ooze. This package has one wavy lamina comprised of silt, and a graded 1 cm-thick bed of silt with an undulose capping layer that is interpreted as a turbidite. The graded

silt bed produces a sharp MS spike and a dark contrast on the x-radiograph, indicating that its composition is different from surrounding sediments (Figure 13). The uppermost lithofacies in the core is a ~6 cm thick package of structureless (homogenous) silty ooze. The MS for the structureless ooze is consistently very low.

Using the paired wood/sediment dates at 40 cm, a correction factor of 4,220 yr. was calculated for the sediment dates. This value represents the difference in age between sediment organic matter and a charred twig recovered from the same horizon. 4,220 years were subtracted from all ages derived from sediment organic matter, to adjust them for contributions of old carbon (the reservoir effect; see also Cohen, 2003). This calibration step resulted in ages that range from 90 – 460 years BP (Table 3). The reservoir effect arises because large lakes are commonly stratified and as a result, older ^{14}C -depleted carbon sources are stored in the hypolimnion (i.e., the lake's deepest layer that is not in contact with the atmosphere) and influences the ambient CO_2 pool (Cohen, 2003). This older carbon may be derived from the weathering of limestone bedrock, older soils, or hydrothermal spring waters, which result in a significant lowering of the initial $^{14}\text{C}/^{12}\text{C}$ value relative to the global mean atmospheric ratio at the time of formation (Cohen, 2003). In addition to the reservoir effect, it is also important to consider that differences in values could be due to an unconformity, but there are no indicators of major erosion surfaces in the core that would support such a conclusion.

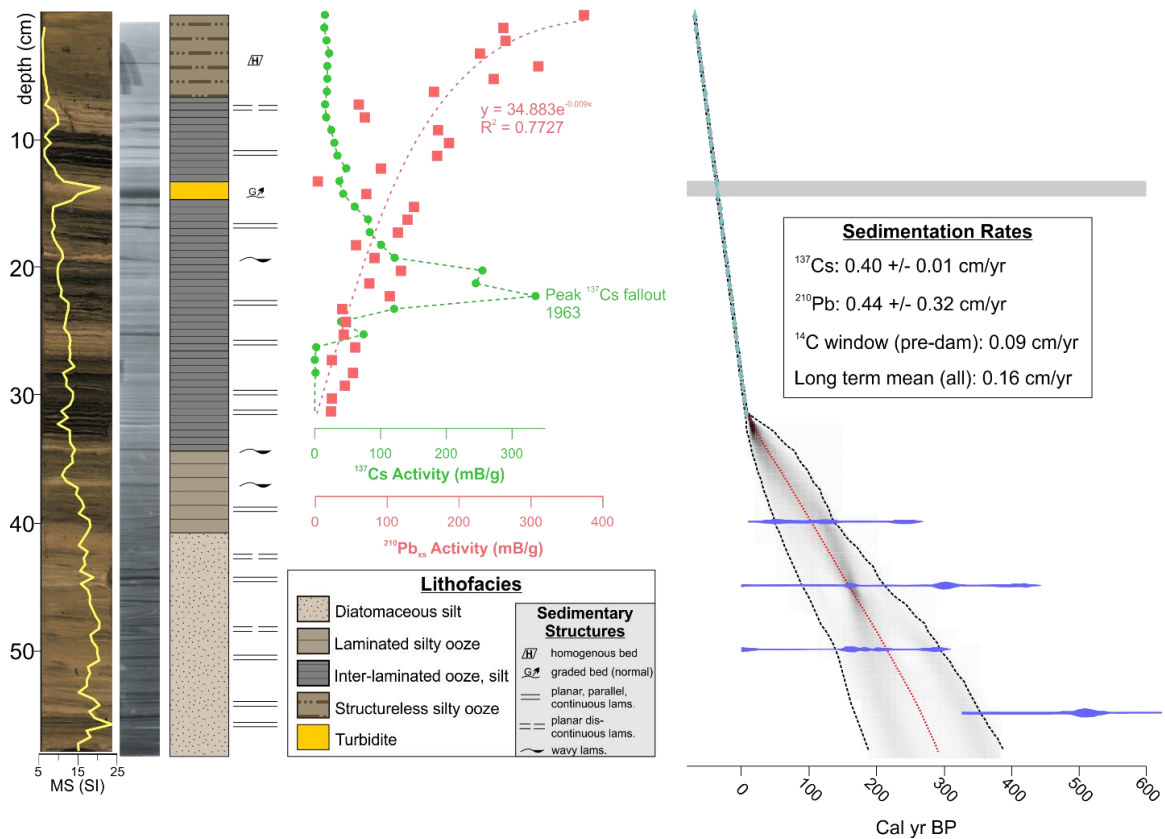


Figure 13: Core 9B stratigraphy, magnetic susceptibility, and age-depth model (from McGlue et al., 2023). The core consists of four different lithofacies. 1) Diatomaceous silt with occasional planar continuous laminae and planar discontinuous laminae. 2) Laminated silty ooze with planar parallel continuous lamina and wavy laminae. 3) Inter-laminated organic-rich ooze (black) and silty ooze (tan) with occasional planar continuous, wavy lamina, and a prominent turbidite at ~13-14 cm. 4) Structureless silty ooze in a homogeneous bed. These lithofacies change from the dam installation both in rate and character.

Sediment Core Chronology

^{210}Pb sedimentation rates

For the 9B sediment core, the $^{210}\text{Pb}_{\text{xs}}$ activities are high (nearly reaching 400 mB/g at the top of the core) and yielded a long chronology. The $^{210}\text{Pb}_{\text{xs}}$ profile exhibited systematic down-core decay to supported levels that were readily interpretable and allowed for the calculation of sediment linear and mass accumulation rates. The mean linear rate

based on the constant rate of supply (CRS) model is 0.44 ± 0.32 cm yr.⁻¹ for the period 1850-2019.

¹³⁷Cs sedimentation rates

For the 9B sediment core, the ¹³⁷Cs activity profile exhibited relatively constant levels with a prominent peak in 1963 coinciding with the Limited Test Ban Treaty between the United States, United Kingdom, and the Soviet Union to stop above-ground nuclear bomb testing. Based on the ¹³⁷Cs data, the sediment accumulation rate at the Jackson Lake 9B site is 0.40 ± 0.01 cm yr.⁻¹ for the period 1850-2019. Therefore, the ¹³⁷Cs and ²¹⁰Pb data show excellent agreement with respect to linear sedimentation rates in the upper ~30 cm of core 9B.

¹⁴C sedimentation rates

Radiocarbon dates for core 9B are listed in Table 3. The conventional radiocarbon ages range from 90 to 4,680 YBP. These ages required correction for reservoir effects because of the large offset between the ages of the charred wood and sediment organic matter collected from the same horizon. Using the paired wood/sediment dates at 40 cm, a correction factor of 4,220 yr. was calculated for the dates on sediment organic matter. This was used for calibration of all the sediment organic matter dates, which results in ages that range from 90 – 460 years BP (Table 3). This technique assumes that the reservoir effect does not change dramatically over time, which we cannot verify with the data that are available. Future research using longer cores may be able to develop additional paired macrofossil-sediment dates, and thus investigate temporal changes in the old carbon reservoir, as has been noted in other large lakes (e.g., Geyh et al., 1997; Felton et al., 2007)

The reservoir effect arises because large lakes are commonly stratified, and older ^{14}C -depleted sources of carbon stored in the hypolimnion (deep layer) influence the ambient CO_2 pool as a result (Cohen, 2003). This older carbon may be derived from the weathering of limestone bedrock, soils, spring waters, or from hydrothermal sources, which result in a significant lowering of the initial $^{14}\text{C}/^{12}\text{C}$ relative to the global mean atmospheric ratio at the time of formation (Cohen, 2003). In the case of Jackson Lake, a hydrothermal spring system that was discovered along the trace of the Teton fault is a likely candidate source for the introduction of ancient, radiocarbon-dead carbon (USGS, 1978).

Bacon Age Model and Sedimentation Rates

Using all the chronometers, a statistical age-depth model for core 9B was developed. The long-term linear sedimentation rate for the core is $\sim 0.16 \text{ cm yr}^{-1}$. The sedimentation rate for the 31.5 - 57.5 cm interval is constrained by ^{14}C dates, at a slower linear rate of $\sim 0.092 \text{ cm yr}^{-1}$. The sedimentation rate for 0 to 31 cm interval is constrained by ^{210}Pb and ^{137}Cs , and averages $\sim 0.41 \text{ cm yr}^{-1}$. The ^{14}C dates span the years 1654-1850. The ^{210}Pb and ^{137}Cs dating covers the years 1906-2019. Thus, a small gap occurs between the radiocarbon and fallout radionuclide dates, and this interval of the age model is the least well-constrained. Nevertheless, an acceleration in sediment accumulation rate moving from the bottom to the top of the core is apparent.

My interpretation from the Bacon age-depth model is that the timeline created for the 9B sediment core reveals four key events in the lake's environmental history. The first key event is the end of the Little Ice Age, in 1850 CE, which appears at $\sim 39 \text{ cm}$ depth. The second key event, the emplacement of the dam from 1905-1922, occurs at 34.5-33 cm. Third, a lake level lowstand in 1986 matches up with the 14-13 cm interval, where a

prominent turbidite has been identified. The final key event was the Nuclear Test Ban Treaty signed in 1963. This treaty ended above ground nuclear bomb testing and ^{137}Cs fallout spiked in 1963, corresponding to ~23 cm, followed by a dramatic decrease in ^{137}Cs levels in sediment.

CHAPTER 5. DISCUSSION

5.1 Overview

The influence of dam installation over the Snake River outlet of Jackson Lake can be observed in several of the maps produced in this study, including the bathymetry, acoustic basement, and total sediment isopach, as well as insights provided by the acoustic facies and sediment characteristics captured in core 9B. Byrd et al. (1994) were among the first researchers to indicate the possible influence of the Teton fault on Jackson Lake. At the time of that study, the Teton fault was believed to extend up to 70 km along the base of the Teton Range (Byrd et al., 1994). More recently, the study of Thigpen et al. (2021) suggested that the Teton fault may extend much farther to the north, but the zone of maximum fault displacement is adjacent to the deepwater depocenter identified in this thesis. The installation of the dam changed Jackson Lake's bathymetry by increasing the base level and causing a lake level transgression, which had a major effect on the size, shape, and position of the Snake River delta at the lake's northern terminus (Figure 1). Completion of the dam made the deepwater areas of Jackson Lake even deeper (today, ~188 ms TWTT, ~141 m maximum depth) and formed new areas of shallow water which are well-expressed in the north (up to ~13 ms TWTT, ~10 m). Another influence of dam installation on water depths can be observed on the lake's eastern margin, where early mapping of landforms revealed the presence of drumlins and other evidence of glacial

erosion and sediment deposition (Pierce et al., 2018). This is an area that was formerly inundated by shallow water or subaerially exposed and is marked by numerous accumulations of glacial sediment that I have interpreted as drumlins and moraines based on their seismic facies characteristics.

The Teton fault initiated in the mid-Miocene, making it far older than the period of glaciation that carved the lake (Brown et al., 2017; Thigpen et al., 2021). That said, the acoustic basement identified in this study is interpreted to be young, most likely of the Quaternary Period. The acoustic basement surface in most areas beneath Jackson Lake is interpreted to have been scoured by the southern margin of the Greater Yellowstone Glacial System that was sourced from the Yellowstone Plateau to the north, in the form of the Snake River lobe (Pierce et al., 2018). The Snake River Lobe is believed to have carved the basin and helped to form accommodation for post-glacial sediments, but it also deposited glacial outwash and moraines in Jackson Hole during the Pleistocene that affected the overall morphology, slope, and hydrology of the region (Pierce et al., 2018). The ages of many of these glacial features located south of Jackson Lake were determined by cosmogenic isotope dating (^{10}Be) applied to exposed boulders in moraines; the current consensus is that the landscape formed ~15.5-14.5 ka (Pierce et al., 2018). This glacial till was transported by the ice sheet resulting in the formation of drumlins on the eastern side of Jackson Lake. The southern margin of the lake was also influenced by glacial deposition, as that area is a terminal moraine that was produced from ice melt (ablation). The acoustic basement reaches a maximum depth of ~311 ms TWT (~233 m assuming a constant interval velocity of 1,500 m sec.⁻¹). The interval velocity calculation uses 1,500 m sec.⁻¹ for soft wet sediments at the lakebed because the sediments usually have low acoustic

impedance values and high porosities making the velocity similar to that of freshwater (Smith et al., 2018). The deepest area of acoustic basement appears to reflect the influence of the Teton fault, as it occupies an area on the western side of the lake in the major depocenter, mirroring the bathymetric map. That said, it remains unknown what the lithological composition of the acoustic basement is across Jackson Lake. In the northern lake axis, the acoustic basement is likely dense, clayey sands deposited by the Snake River; clearly the CHIRP profiler was unable to penetrate deep into these sediments due to their composition. In this area of the lake, acoustic basement does not equate to the geological basement or the pre-rift basin transition. In contrast, acoustic basement in the depocenter could be glacial deposits. Faint parabolic and irregular reflections deep in the center of the lake's stratal package could be related to the presence of diamictic sediments, perhaps with some large boulders that generate diffractions in the seismic reflection data. If long coring can be accomplished in the lake, it could be possible to acquire ground truth that will clarify the composition of the acoustic basement deposits.

The total sediment isopach map is the calculated difference between the acoustic basement and the bathymetric maps, which provides insights on the sediment thickness and the spatial distribution of glacial and post-glacial sediments in Jackson Lake. The maximum thickness is ~155 ms TWTT, and this occurs in the deepwater depocenter. The sediment package of the depocenter truncates against the Teton fault in the west without major thickening. This is opposite to Bear Lake in Utah-Idaho, another lake that is situated in a seismically active rift basin (Colman, 2006). There, the strata thicken towards the large, basin-bounding border fault. Bear Lake also has a clinoformal paleo delta package in the northern section of the lake and provides a partial analogue for Jackson Lake (Colman,

2006). The depocenter sediment package thins to the north and southwest, though the bays (e.g., Moran, Bearpaw, Spaulding) have 10s of ms TWTT of well-imaged sediment. The acoustic thickness of the sediment package appears to thin towards the Snake River delta in Jackson Lake, and the source of the sediments in this area is from weathered rocks of the Snake River volcanic plateau and other lithologies in the headwaters of the Snake River. That said, acoustic imaging in the northern end of Jackson Lake was challenging, and most images from the area show a shallow water bottom multiple in the sub-surface just below the lake floor reflector. This is interpreted to be an effect of the coarse, clayey sands in the Snake River delta that were less amenable to deep imaging with the high frequency CHIRP source, which makes a big contrast with the lower density hemipelagic lake sediments found in the depocenters.

5.2 Evidence of Dam Installation from Seismic Facies

Five shallow acoustic facies (AF) were identified on the Jackson Lake floor (Table 4), and several of these facies have been influenced by the transgression associated with the installation of Jackson Lake Dam in the early 20th century.

1. **Tabular or Sheet-like (AF-1)**

AF-1 is mostly restricted to the northern axis of Jackson Lake, where the present-day Snake River delta is forming. By definition, a delta is a fan-shaped sedimentary plain that appears near the mouth of a river following an alluvial tract, and a lacustrine delta is a specific type of delta that forms in a lake. The Snake River delta plain can be seen in the acoustic facies as high amplitude, parallel, semicontinuous lake floor returns with occasional discontinuous reflections. AF-1 is interpreted as a submerged paleo-delta plain, floodplain, or lake margin deposits. These features generally follow the basal surface of

the underlying topography. The discontinuous areas are interpreted to be a result of channels cutting the meanders on the drowned Snake River delta plain, which appear prominently on maps and satellite images of the lake when water levels are low (e.g., Dilworth et al., 2023). The evidence for the Snake River delta is limited to the northern end of the lake in what is today a shallow water area. A similar analogue includes a study conducted by Baster et al. (2003) in western Lake Geneva (Switzerland) that used high resolution seismic profiles and sediment cores to study seismic stratigraphy's role in the evolution of Lake Geneva's Promethous delta. There, the submerged delta plain also appeared in seismic profiles as moderate-high amplitude reflections, similar to the northern end of Jackson Lake.

2. Clinoforms (AF-3)

Climoforms are chronostratigraphic, sloped stratal depositional surfaces corresponding to past lake level profiles that are often created by deltas over periods of 10^3 - 10^5 years (Patruno and Hansen, 2018). The internal acoustic characteristics of the clinoforms in Jackson Lake are low-moderate amplitude, sharply oblique to complex sigmoid-oblique, prograding reflections. AF-3 is found in the northern end of the lake and along the bays (Moran and Snowshoe Canyons and at Second and Pilgrim Creeks) at the southern end of the lake. These packages can be traced updip to nearby mouths of the rivers and I named them accordingly, because without the transgression caused by the dam installation these rivers would still likely connect to the now-submerged delta complexes. The clinoforms found were associated with the Snake River, Arizona Creek/Bailey Creek, North Moran Creek and Moran Creek, and Pilgrim Creek/Second Creek/Third Creek (Figure 8). These are useful for identifying base level change, because the topset-to-foreset

transition is a quantitative marker of prior water level (Steel and Olsen, 2002). The clinoforms found in Jackson Lake share a number of acoustic similarities to those found in a study done in Lake Malawi (Lyons et al. 2011). Lyons et al. (2011) conducted a stratigraphic analysis integrating drill-core and seismic-reflection data for Lake Malawi, a large, multi-segment rift lake in the African Rift Valley. The data presented by Lyons et al. (2011) were useful as an analogue because the Lake Malawi seismic profiles clearly imaged the internal geometry of progradational delta facies, which were sigmoidal or oblique clinoform packages. While both lakes have experienced rapid lake-level change, Lake Malawi has low-stands due to severe aridity and semi-desert conditions; such conditions likely did not affect Jackson Lake since the Pinedale glaciation. Comparable to Lake Malawi's facies, another rift basin in eastern Africa, Lake Edward, shows similar facies in a much simpler depositional system consisting of a single half-graben segment, perhaps more akin to Jackson Lake (McGlue et al., 2006). Specifically in Lake Edward, McGlue et al. (2006) identified and interpreted progradational delta facies, with low-amplitude, discontinuous reflections in packages of oblique or sigmoid clinoforms reflections that make a clear analogue for what is seen in Jackson Lake. In the Lake Malawi and Lake Edward analogs, the deltaic clinoforms were interpreted to result from lake level changes, with the sediments accumulating when base level was lower than modern conditions, and transgression led to burial of these features with hemipelagic sediments.

3. Mounds (AF-4)

A drumlin is an oval-shaped hill, mound, or ridge composed of glacial till that appears smooth and elongated in plan view. Drumlins form under the ice margin and are shaped by glacial flow. The long axis of the feature is usually parallel or sub-parallel to the

direction of ice movement (Bates et al., 1984; Neuendorf et al., 2005). In Jackson Lake, I interpret AF-4 to be submerged drumlins. The seismic characteristics of these features are high amplitude, continuous to discontinuous lake floor returns with minimal internal reflections. These are primarily found along the eastern side of the lake where water depths are shallower, and a number of these features create positive bathymetric relief. The scale of these mounds ranges from ~130 to 2,000 m along the long axis. These features appear to be an offshore continuation of the set of drumlins that form a field onshore. Pierce et al. (2018) remarked that the eastern side of Jackson Lake, in the area of Colter Bay, is a large tract of terrain formed by basal sliding of the Pinedale glacier. The elongated depressions from the glacial scouring made many of the bays of Jackson Lake (Pierce et al., 2018). The drumlin topography is illustrated in Figure 14 (Pierce et al., 2018). The drumlins in Jackson Lake are similar in shape, size, and acoustic characteristics to drumlins imaged in Oneida Lake in New York (Zaremba and Scholz, 2021). The deformed shape of the drumlins can be explained by sediment reworking or erosion, which can be facilitated by slope failure, wave action, or a changing water levels (Zaremba and Scholz, 2021).

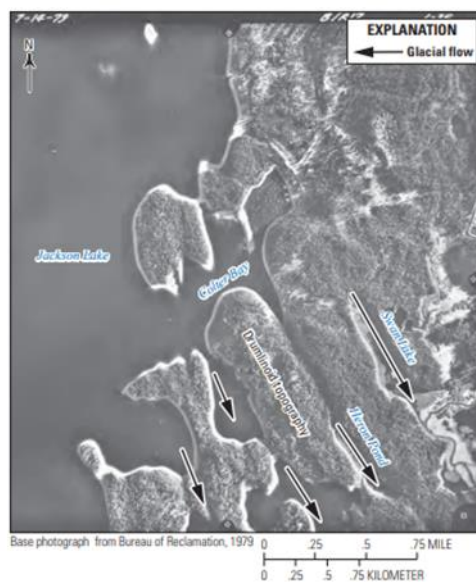


Figure 14: Drumlin morphology from Pierce et al. (2018), showing features subaerially exposed on the east side of Jackson Lake. They formed during the Pinedale stage 2 and 3 by the Snake River lobe. The ice moved southeast across this section of the lake.

4. Basin-Fill (AF-2)

I interpret the basin fill facies that occurs across much of the Jackson Lake depocenter to represent hemipelagic lacustrine sediments. Hemipelagic sediments are fine-grained biogenic and terrigenous particles that settle to the lake floor from the water column under the influence of gravity (Ochoa et al., 2013). AF-2 consists of low to moderate amplitude, moderate-frequency reflections. Reflections appear predominantly continuous interspersed with occasional divergent, chaotic reflections. The basin-fill can be subdivided into two separate facies types. The first is characterized by parallel basin-fill reflections and the second is marked by divergent, chaotic reflections, interpreted to be derived from mass wasting from the steep margins. Analogous basin fill deposits were reported by Praet et al.'s (2016) study of Eklutna and Skilak Lakes (Alaska); both lakes provided seismic evidence for thin hemipelagic drape deposits that blanket the basin floor and moderately steep basin margin. In that study, the relatively uniform succession of horizontally stratified, low-high amplitude seismic facies are termed “background sedimentation” (Praet et al., 2016). Another analogue exists in Fallen Leaf Lake, which sits in the Lake Tahoe Basin (Maloney et al., 2013). Maloney et al. (2013) used seismic profiles to identify slide deposits (debris flows and turbidites), which appear as divergent, chaotic reflections that infill topographic lows in a lenticular shape.

5. Slope Front (AF-5)

Slope-front facies appear as a hard lake floor seismic reflection return with multiple underlying shallow diffractions. Internal reflectivity and sub-bottom penetration are

minimal. AF-5 is limited to areas adjacent to the steep trace of the Teton fault, and I therefore interpret this acoustic response to be generated by exposed (or nearly so; some areas may have a thin veneer of sediment cover), steeply dipping bedrock. In the study of Larsen et al. (2016) of Jenny Lake, another nearby moraine-bound glacial lake in Grant Teton National Park, topographic highs that were acoustically opaque on the seismic profiles were interpreted as Teton fault scarps (Larsen et al., 2016); these features share some similarities to the AF-5 facies. In the Lake Tahoe Basin at Fallen Leaf Lake, Maloney et al. (2013) described a large topographic high near the modern scarp of the West Tahoe-Dollar Point fault with little to no lacustrine sediment draping the steep basin walls, which also looks similar to the slope front facies in Jackson Lake.

5.3 Evidence from Sediment Core 9B

6. Changes in sedimentation rates

The sedimentation rate for the interval from 31.5 to 57.5 cm is constrained by ^{14}C dates and exhibits a long-term linear rate of 0.092 cm yr^{-1} . This is a lower rate than the overlying ~31 cm interval constrained via ^{210}Pb and ^{137}Cs , which accumulated at an average of $\sim 0.41 \text{ cm yr}^{-1}$. The emplacement of the dam occurred from 1906-1916 CE, which aligns with the 34.5-33 cm horizon downcore. It is important to note that there is a gap in the age control between the ^{210}Pb and ^{137}Cs and the ^{14}C dates, which makes it difficult to precisely pinpoint when the change in accumulation rate began. That said, it is consistent with changes to the Jackson Lake basin observed in seismic data that dam installation could have increased sedimentation rates at the 9B core site. This is because the lake's major source of sediment, the Snake River, had its delta flooded and transgressed when the dam was installed; this may have resulted in remobilization of previously subaerial clayey

sediments and organic matter. Hambright et al. (2004) gave a similar account of the impact of dam installation raising sedimentation rates in Lake Kinneret in Israel. Lake Kinneret experienced this increased sediment flux during periods of ecosystem destabilization, for example when the lake transitioned into a National Water Carrier, and when nearby, hydrologically connected lake and swamps were drained (Hambright et al., 2004). These water-level fluctuations contributed to accelerated eutrophication and an increase in bulk sedimentation as phosphorus was loaded into the system. This is similar to Jackson Lake; the organic richness of the core 9B sediments increased following dam installation, which McGlue et al. (2023) attributed to a change in trophic state as lake margin wetlands and terrestrial vegetation were submerged by rising lake levels.

7. Changes in lithofacies

The chronology of core 9B devised from the Bacon age-depth model allows me to pinpoint the stratal interval of dam installation, which was ~34.5-33 cm. Interestingly, there is a significant lithofacies change in the core at this depth. The core changed from laminated silty ooze into the black inter-laminated organic-rich oozes and tan silty oozes. This facies appeared as water level elevation increased following dam installation, and then the black organic-rich sediments appeared cyclically as highstands occurred on the lake-level curve (McGlue et al., 2023). The lithofacies prior to dam installation included wavy laminations which switched into planar, parallel continuous laminations after dam emplacement. Hambright et al. (2004) discusses a large influx of phosphorus after the dam installation, which caused an acceleration in eutrophication in Lake Kinneret. A similar process may have occurred in Jackson Lake, as the Snake River delta was flooded and deltaic and lake margin vegetation decomposed and released nutrients to the water column. This

interpretation is supported by diatom assemblages published by Dilworth et al. (2023). According to Friedl and Wüest (2002), the consequences of impoundment of natural lakes by dams includes increased water residence time, water temperature, water column stratification, and reductions in turbidity. Those authors also noted that dams can sometimes result in an increase in primary production and shoreline erosion. Additionally, Friedl and Wüest (2002) noted that for lakes like Jackson Lake, seasonal changes in hydrological regime will affect the natural biogeochemical cycles of carbon, nutrients, and metals, shifting them from allochthonous to autochthonous.

CHAPTER 6. CONCLUSIONS

6.1 Conclusions

Seismic reflection surveys and a short gravity core conducted on and collected from Jackson Lake in 2018-2019 led to several new discoveries about this depositional basin. Seismic reflection profiles resulted in the construction of a new bathymetric map that showed one large and deep depocenter covering an area of $\sim 25 \text{ km}^2$, stretching from the area offshore of Colter Canyon to an area southwest of Elk Island, adjacent to Moran Bay. The deepwater depocenter has a boot-like morphology that tapers to the south, and a maximum depth of $\sim 183 \text{ ms TWTT}$. A secondary depocenter was also discovered, and it exhibited a maximum depth of $\sim 53 \text{ ms TWTT}$. This secondary depocenter is $\sim 7.6 \text{ km}^2$ in area and it is situated below Donoho Point, extending from northeastern Spaulding Bay to the area offshore from Pilgrim Creek near the Jackson Lake Dam on the southeastern side of the lake. Another significant new finding of this research was the depth to acoustic basement, which in plan view takes on a similar pattern to the bathymetry. The maximum

depth of the acoustic basement horizon is ~311 ms TWTT. Like the bathymetry map, the acoustic basement defines the main depocenter, which is controlled by several normal faults. There are two normal faults on the western side of the depocenter and four candidate normal faults on the eastern side, which form an uplifted, shallow water platform. The candidate normal faults on the eastern side of the lake exhibit lower dip angles than those to the west, which makes their identification a challenge. Alternatively, the steep-sided nature of the lake's eastern margin could be a function of glacial erosion. The normal fault on the western side of the basin is likely the Teton fault, or another large, down-to-the-east normal fault synthetic to the Teton fault.

An isopach map constructed from the bathymetric and acoustic basement maps defines the sediment thickness in Jackson Lake. There is a thick sediment package in the main depocenter that averages ~116 ms TWTT thick with a maximum thickness of 155 ms TWTT and a second depocenter with a sediment package that reaches ~97 ms TWTT thick in the center. There is a shallow area in the northern end of the lake whose morphology and sediment thickness are a function of the dam installation, as this area would otherwise be subaerially exposed. Prior to dam installation, this was the location of the Snake River delta plain.

This study revealed five shallow seismic facies: (a) tabular/sheet-like, (b) basin fill, (c) clinoform, (d) mound, and (e) slope front. In the seismic dataset, there are four distinct clinoform packages, which have been interpreted as drowned paleo-deltas. These are the Snake River paleo-delta, Arizona Creek/Bailey Creek paleo-delta, Pilgrim Creek/Second Creek paleo-delta, and the Moran Bay paleo-delta. The installation of Jackson Lake Dam raised the water level by ~12 m, which is the position of the topset-to-foreset transition of

these clinoforms. Other evidence of transgression associated with dam installation is submerged glacial features, including prominent mound-like packages in shallow water, which we interpret as drumlins.

We additionally studied a short gravity core using ^{137}Cs , ^{210}Pb , and ^{14}C in order to ascertain deepwater sedimentation rates and lithofacies. The core analyzed in this study was collected from the deepwater depocenter, an area characterized by low-moderate amplitude, continuous seismic reflections, which suggest mostly hemipelagic depositional processes. The lithofacies identified in the core confirmed this interpretation, as well as showing some intriguing variability in depositional processes that implicate the influence of climate change and dam emplacement in Jackson Lake. The bottom (chronologically oldest) of the core record was dominated by diatomaceous silt that accumulated near the termination of the Little Ice Age, a period of minor glacial advance in western Wyoming that ended in the late 19th century. A marked shift occurred in deepwater sedimentation following the installation of the dam; the datum (~1906-1916 CE) coincides with both increases in organic matter-rich sedimentation (e.g., laminated black oozes) and accumulation rates. High-resolution water level elevation data from the Bureau of Reclamation indicates that organic matter accumulation in Jackson Lake following the construction of the dam varied with lake level, with highstands (lowstands) showing high (low) relative concentrations of TOC (McGlue et al., 2023). I interpret the increase in carbonaceous sedimentation following the dam construction to have resulted from nutrient loading, which was probably caused by flooding and decomposition of nearshore vegetation as water levels rose. Another interesting aspect of the core lithofacies was the presence of a cm-scale belt of graded silt in the late 1980s, which I interpreted to be a

turbidite. This feature was deposited during a lake level lowstand, and therefore provides valuable evidence for the scale and sedimentological composition of gravity flow deposits that affect Jackson Lake as water levels decline.

These lithofacies change from the dam installation both in rate and character. After the dam was installed, I interpreted using the Bacon model that the facies switched to black laminated sediments interbedded with tan silty clays with sedimentation rates changing from 0.09 cm yr.^{-1} pre-dam to $0.40\text{-}0.44 \text{ cm yr.}^{-1}$ post-dam. The derived geochronology ranges from 1658-2019 CE. Future work on Jackson Lake should focus on the collection of a long core, in order to test changes in sedimentation rate and lithofacies over longer time periods; this should help to resolve the history of earthquakes and climate change in the region.

REFERENCES

- ACHARYA, A., PIECHOTA, T. C. & TOOTLE, G. 2012. Quantitative assessment of climate change impacts on the hydrology of the North Platte River watershed, Wyoming. *Journal of Hydrologic Engineering*, 17, 1071-1083.
- ANDERSON, J. G. & BIASI, G. P. 2016. What is the basic assumption for probabilistic seismic hazard assessment? *Seismological Research Letters*, 87, 323-326.
- APPLEBY, P. & OLDFIELDZ, F. 1983. The assessment of ^{210}Pb data from sites with varying sediment accumulation rates. *Hydrobiologia*, 103, 29-35.
- BASTER, I., GIRARD-CLOS, S., PUGIN, A.J., & WILDI, W. 2003. High-resolution seismic stratigraphy of an Holocene lacustrine delta in western Lake Geneva (Switzerland). *Eclogae Geologicae Helvetiae*, 96, 11-20.
- BATES, R. L., AND J. A. JACKSON, EDITORS. 1984. Dictionary of geological terms. Third edition. American Geological Institute, Alexandria, Virginia.
- BEHRENDT, J. C., TIBBETTS, B. L., BONINI, W. E., LAVIN, P. M., LOVE, J. & REED, J. C. 1968. A geophysical study in Grand Teton National Park and Vicinity, Teton County, Wyoming: With sections on stratigraphy and structure and precambrian rocks. US Geological Survey.
- BLAAUW, M. & CHRISTEN, J. A. 2011. Flexible paleoclimate age-depth models using an autoregressive gamma process. *Bayesian analysis*, 6, 457-474.
- BRACHT, B. B., STONE, J. R. & FRITZ, S. C. 2008. A diatom record of late Holocene climate variation in the northern range of Yellowstone National Park, USA. *Quaternary International*, 188, 149-155.
- BROWN, S. J., THIGPEN, J. R., SPOTILA, J. A., KRUGH, W. C., TRANEL, L. M. & ORME, D. A. 2017. Onset timing and slip history of the Teton fault, Wyoming: A multidisciplinary reevaluation. *Tectonics*, 36, 2669-2692.

BUREAU OF RECLAMATION (ed.). 2018 Minidoka Project, Bureau of Reclamation. Available at: <https://www.usbr.gov/projects/index.php?id=361> (Accessed: 25 May 2023).

BYRD, J. O. D. 1995. *Neotectonics of the Teton fault, Wyoming*, The University of Utah.

BYRD, J.O., SMITH, R.B. AND GEISSMAN, J.W. 1994. The Teton fault, Wyoming: Topographic signature, neotectonics, and mechanisms of deformation. *Journal of Geophysical Research: Solid Earth*, 99(B10), pp.20095-20122.

CALAYIR, Y. & KARATON, M. 2005. Seismic fracture analysis of concrete gravity dams including dam-reservoir interaction. *Computers & Structures*, 83, 1595-1606.

CARROLL, A. R. & BOHACS, K. M. 1999. Stratigraphic classification of ancient lakes: Balancing tectonic and climatic controls. *Geology*, 27, 99-102.

CASE, J. C., TONER, R. N. & KIRKWOOD, R. 2002. Basic Seismological Characterization for Teton County, Wyoming (Exclusive of Yellowstone National Park).

CHILDS, J. R., SNYDER, N. P. & HAMPTON, M. A. 2003. Bathymetric and geophysical surveys of Englebright Lake, Yuba-Nevada Counties, California.

COHEN, A. S. 2003. *Paleolimnology: the history and evolution of lake systems*, Oxford university press.

COLMAN, S.M. 2006. Acoustic stratigraphy of Bear Lake, Utah–Idaho—Late Quaternary sedimentation patterns in a simple half-graben. *Sedimentary Geology*, 185(1-2), pp.113-125.

- DELAUNE, R., PATRICK, W. & BURESH, R. 1978. Sedimentation rates determined by ^{137}Cs dating in a rapidly accreting salt marsh. *Nature*, 275, 532-533.
- DILWORTH J, STONE JR, YEAGER KM, THIGPEN JR AND MCGLUE MM. 2023. Fossil Diatoms Reveal Natural and Anthropogenic History of Jackson Lake (Wyoming, USA). *Earth Sci. Syst. Soc.* 3:10065. doi: 10.3389/esss.2023.10065
- DUROSS, C. B., GOLD, R. D., BRIGGS, R. W., DELANO, J. E., OSTENAA, D. A., ZELLMAN, M. S., CHOLEWINSKI, N., WITKE, S. J. & MAHAN, S. A. 2020. Holocene earthquake history and slip rate of the southern Teton fault, Wyoming, USA. *Bulletin*, 132, 1566-1586.
- EGAN, T. 2005. The Worst Hard Time: The Untold Story of Those Who Survived the Great American Dust Bowl, The Dust Bowl, National Drought Mitigation Center. Available at: <https://drought.unl.edu/dustbowl/> (Accessed: 25 May 2023).
- FELTON, A.A., RUSSELL, J.M., COHEN, A.S., BAKER, M.E., CHESLEY, J.T., LEZZAR, K.E., MCGLUE, M.M., PIGATI, J.S., QUADE, J., STAGER, J.C. AND TIERCELIN, J.J., 2007. Paleolimnological evidence for the onset and termination of glacial aridity from Lake Tanganyika, Tropical East Africa. *Palaeogeography, Palaeoclimatology, Palaeoecology*, 252(3-4), pp.405-423.
- FORD, S. 2020. Jackson Lake Dam, Jackson Hole Historical Society & Museum. Available at: <https://jacksonholehistory.org/jackson-lake-dam/> (Accessed: 25 May 2023).
- FRANKSON, R., K.E. KUNKEL, L.E. STEVENS, D.R. EASTERLING, B.C. STEWART, N.A. UMPHLETT, AND C.J. STILES, 2022: Wyoming State Climate Summary 2022. NOAA Technical Report NESDIS 150-WY. NOAA/NESDIS, Silver Spring, MD, 5 pp.
- FRIEDL, G. AND WÜEST, A. 2002. Disrupting biogeochemical cycles-Consequences of damming. *Aquatic Sciences*, 64, pp.55-65.
- GEYH, M.A., SCHOTTERER, U. AND GROSJEAN, M., 1997. Temporal changes of the ^{14}C reservoir effect in lakes. *Radiocarbon*, 40(2), pp.921-931.

- HAMBRIGHT, K.D., ECKERT, W., LEAVITT, P.R. AND SCHELSKE, C.L. 2004. Effects of historical lake level and land use on sediment and phosphorus accumulation rates in Lake Kinneret. *Environmental science & technology*, 38(24), pp.6460-6467.
- HANSEN, K. 2017. Meeting the Challenge of Water Scarcity in the Western United States. *Competition for Water Resources*. Elsevier.
- HERSCHY, R. W. 2012. Dams, Classification. In: BENGTSSON, L., HERSCHY, R. W. & FAIRBRIDGE, R. W. (eds.) *Encyclopedia of Lakes and Reservoirs*. Dordrecht: Springer Netherlands.
- HOLECHEK, J.L., GELI, H.M., CIBILS, A.F. AND SAWALHAH, M.N., 2020. Climate change, rangelands, and sustainability of ranching in the Western United States. *Sustainability*, 12(12), p.4942.
- KILHAM, S. S., THERIOT, E. C. & FRITZ, S. C. 1996. Linking planktonic diatoms and climate change in the large lakes of the Yellowstone ecosystem using resource theory. *Limnology and Oceanography*, 41, 1052-1062.
- KOTTEK, M., GRIESER, J., BECK, C., RUDOLF, B. AND RUBEL, F. 2006. World map of the Köppen-Geiger climate classification updated.
- LARSEN, D. J., CRUMP, S. E., ABBOTT, M. B., HARBERT, W., BLUMM, A., WATTRUS, N. J. & HEBBERGER, J. J. 2019. Paleoseismic evidence for climatic and magmatic controls on the Teton Fault, WY. *Geophysical Research Letters*, 46, 13036-13043.
- LARSEN, D. J., FINKENBINDER, M. S., ABBOTT, M. B. & OFSTUN, A. R. 2016. Deglaciation and postglacial environmental changes in the Teton Mountain Range recorded at Jenny Lake, Grand Teton National Park, WY. *Quaternary Science Reviews*, 138, 62-75.
- LYONS, R.P., SCHOLZ, C.A., BUONICONTI, M.R. AND MARTIN, M.R. 2011. Late Quaternary stratigraphic analysis of the Lake Malawi Rift, East Africa: An integration of drill-core and seismic-reflection data. *Palaeogeography, Palaeoclimatology, Palaeoecology*, 303(1-4), pp.20-37.

- MALONEY, J.M., NOBLE, P.J., DRISCOLL, N.W., KENT, G.M., SMITH, S.B., SCHMAUDER, G.C., BABCOCK, J.M., BASKIN, R.L., KARLIN, R., KELL, A.M. AND SEITZ, G.G. 2013. Paleoseismic history of the Fallen Leaf segment of the West Tahoe–Dollar Point fault reconstructed from slide deposits in the Lake Tahoe Basin, California–Nevada. *Geosphere*, 9(4), pp.1065-1090.
- MANN, M. E., ZHANG, Z., RUTHERFORD, S., BRADLEY, R. S., HUGHES, M. K., SHINDELL, D., AMMANN, C., FALUVEGI, G. & NI, F. 2009. Global signatures and dynamical origins of the Little Ice Age and Medieval Climate Anomaly. *Science*, 326, 1256-1260.
- MANTUA, N. J. 1999. The Pacific decadal oscillation and climate forecasting for North America. *Climate Risk Solutions*, 1, 10-13.
- MARSTON, R. A., MILLS, J. D., WRAZIEN, D. R., BASSETT, B. & SPLINTER, D. K. 2005. Effects of Jackson Lake Dam on the Snake River and its floodplain, Grand Teton National Park, Wyoming, USA. *Geomorphology*, 71, 79-98.
- MCGLUE, M. M., DILWORTH, J. R., JOHNSON, H. L., WHITEHEAD, S. J., THIGPEN, J. R., YEAGER, K. M., WOOLERY, E. W., BROWN, S. J., JOHNSON, S. E. & CEARLEY, C. S. 2023. Effect of Dam Emplacement and Water Level Changes on Sublacustrine Geomorphology and Recent Sedimentation in Jackson Lake, Grand Teton National Park (Wyoming, United States). *Earth Science, Systems and Society*, 2.
- MCGLUE, M. M., SCHOLZ, C. A., KARP, T., ONGODIA, B. & LEZZAR, K. E. 2006. Facies architecture of flexural margin lowstand delta deposits in Lake Edward, East African Rift: constraints from seismic reflection imaging. *Journal of Sedimentary Research*, 76, 942-958.
- MEKONNEN, MESFIN M., AND ARJEN Y. HOEKSTRA. "Four billion people facing severe water scarcity." *Science advances* 2, no. 2 (2016): e1500323.
- MOERNAUT, J., DAELE, M. V., HEIRMAN, K., FONTIJN, K., STRASSER, M., PINO, M., URRUTIA, R. & DE BATIST, M. 2014. Lacustrine turbidites as a tool for quantitative

- earthquake reconstruction: New evidence for a variable rupture mode in south central Chile. *Journal of geophysical research. Solid earth*, 119, 1607-1633.
- MOERNAUT, J., VAN DAELE, M., STRASSER, M., CLARE, M. A., HEIRMAN, K., VIEL, M., CARDENAS, J., KILIAN, R., DE GUEVARA, B. L. & PINO, M. 2017. Lacustrine turbidites produced by surficial slope sediment remobilization: a mechanism for continuous and sensitive turbidite paleoseismic records. *Marine Geology*, 384, 159-176.
- NAFTZ, D. L., KLUSMAN, R., MICHEL, R. L., SCHUSTER, P. F., REDDY, M., TAYLOR, H. E., YANOSKY, T. & MCCONNAUGHEY, E. 1996. Little Ice Age evidence from a south-central North American ice core, USA. *Arctic and Alpine Research*, 28, 35-41.
- NEUENDORF, K. K. E., J. P. MEHL JR., AND J. A. JACKSON. 2005. Glossary of geology. Fifth edition. American Geological Institute, Alexandria, Virginia.
- OCHOA, J., WOLAK, J. AND GARDNER, M.H. 2013. Recognition criteria for distinguishing between hemipelagic and pelagic mudrocks in the characterization of deep-water reservoir heterogeneity. *AAPG bulletin*, 97(10), pp.1785-1803.
- PATRUNO, S. AND HELLAND-HANSEN, W. 2018. Clinoforms and clinoform systems: Review and dynamic classification scheme for shorelines, subaqueous deltas, shelf edges and continental margins. *Earth-Science Reviews*, 185, pp.202-233.
- PEKAU, O. A., LINGMIN, F. & CHUHAN, Z. 1995. Seismic fracture of koyana dam: Case study. *Earthquake Engineering & Structural Dynamics*, 24, 15-33.
- PIERCE, K. L. & GOOD, J. D. 1992. Field guide to the Quaternary geology of Jackson Hole, Wyoming. US Dept. of the Interior, US Geological Survey.
- PIERCE, K. L., LICCIARDI, J. M., GOOD, J. M. & JAWOROWSKI, C. 2018. Pleistocene glaciation of the Jackson Hole area, Wyoming. US Geological Survey.

- PRAET, N., MOERNAUT, J., VAN DAELE, M., BOES, E., VANDEKERKHOVE, E., STRUPLER, M., HAEUSSLER, P. & DE BATIST, M. 2016. Sublacustrine landslides in several Alaskan lakes reveal a long history of strong earthquake shaking. *GB2016*, 133.
- PRAET, N., VAN DAELE, M., COLLART, T., MOERNAUT, J., VANDEKERKHOVE, E., KEMPF, P., HAEUSSLER, P. J. & DE BATIST, M. 2020. Turbidite stratigraphy in proglacial lakes: Deciphering trigger mechanisms using a statistical approach. *Sedimentology*, 67, 2332-2359.
- ROCHNER, M. L., HEETER, K. J., HARLEY, G. L., BEKKER, M. F. & HORN, S. P. 2021. Climate-induced treeline mortality during the termination of the Little Ice Age in the Greater Yellowstone Ecoregion, USA. *The Holocene*, 31, 1288-1303.
- SCHLAGER, E. & HEIKKILA, T. 2011. Left high and dry? Climate change, common-pool resource theory, and the adaptability of western water compacts. *Public Administration Review*, 71, 461-470.
- SCHNURRENBERGER, D., RUSSELL, J. & KELTS, K. 2003. Classification of lacustrine sediments based on sedimentary components. *Journal of Paleolimnology*, 29, 141-154.
- SCHOLZ, C. A. 2002. Applications of seismic sequence stratigraphy in lacustrine basins. *Tracking environmental change using lake sediments*. Springer.
- SCHOLZ, C. A., JOHNSON, T. C. & MCGILL, J. W. 1993. Deltaic sedimentation in a rift valley lake: new seismic reflection data from Lake Malawi (Nyasa), East Africa. *Geology*, 21, 395-398.
- SHOTBOLT, L. A., THOMAS, A. D. & HUTCHINSON, S. M. 2005. The use of reservoir sediments as environmental archives of catchment inputs and atmospheric pollution. *Progress in physical geography*, 29, 337-361.
- SMITH, R. B., BYRD, J. O. & SUSONG, D. 1990. Neotectonics and structural evolution of the Teton fault. *Geologic field tours of western Wyoming and parts of adjacent Idaho, Montana, and Utah: Geological Survey of Wyoming Public Information Circular*, 126-138.

- SMITH, A.M., WOODWARD, J., ROSS, N., BENTLEY, M.J., HODGSON, D.A., SIEGERT, M.J. AND KING, E.C. 2018. Evidence for the long-term sedimentary environment in an Antarctic subglacial lake. *Earth and Planetary Science Letters*, 504, pp.139-151.
- SNYDER, N. P., WRIGHT, S. A., ALPERS, C. N., FLINT, L. E., HOLMES, C. W. & RUBIN, D. M. 2006. Reconstructing depositional processes and history from reservoir stratigraphy: Englebright Lake, Yuba River, northern California. *Journal of Geophysical Research: Earth Surface*, 111.
- STEEL, R. AND OLSEN, T. 2002. Clinoforms, clinoform trajectories and deepwater sands.
- STENE, E. A. & PROGRAM, U. S. B. O. R. H. 1993. *The Minidoka Project*, Bureau of Reclamation History Program.
- STRASSER, M., MONECKE, K., SCHNELLMANN, M. & ANSELMETTI, F. S. 2013. Lake sediments as natural seismographs: A compiled record of Late Quaternary earthquakes in Central Switzerland and its implication for Alpine deformation. *Sedimentology*, 60, 319-341.
- THIGPEN, R., BROWN, S. J., HELFRICH, A. L., HOAR, R., MCGLUE, M., WOOLERY, E., GUENTHNER, W. R., SWALLOM, M. L., DIXON, S. & GALLEN, S. 2021. Removal of the Northern Paleo-Teton Range along the Yellowstone Hotspot Track. *Lithosphere*, 2021.
- THOMSON, A. M., BROWN, R. A., ROSENBERG, N. J., SRINIVASAN, R. & IZAURRALDE, R. C. 2005. Climate change impacts for the conterminous USA: an integrated assessment. *Climatic change*, 69, 67-88.
- TWICHELL, D. C., CROSS, V. A., HANSON, A. D., BUCK, B. J., ZYBALA, J. G. & RUDIN, M. J. 2005. Seismic architecture and lithofacies of turbidites in Lake Mead (Arizona and Nevada, USA), an analogue for topographically complex basins. *Journal of Sedimentary Research*, 75, 134-148.

U.S. COMMITTEE ON LARGE DAMS. 2000. Observed performance of dams during earthquakes volume II. Available at: http://www.usdams.org/wp-content/uploads/2016/05/ObservedPerformanceII_V2.pdf

USGS, 1978. Report Number: 1100 U. S. G. Survey

DOI: 10.3133/pp1100 Page 56-57

<http://pubs.er.usgs.gov/publication/pp1100>

USGS 13010065 SNAKE RIVER AB JACKSON LAKE AT FLAGG RANCH WY, 2023. NWIS Site Information for USA: Site Inventory. Available at: https://waterdata.usgs.gov/usa/nwis/inventory/?site_no=13010065&agency_cd=USGS (Accessed: 25 May 2023).

USGS 13010500 JACKSON LAKE NEAR MORAN, WY, 2023. USGS Surface-Water Daily Data for the Nation. Available at: https://waterdata.usgs.gov/nwis/dv/?referred_module=sw&site_no=13010500 (Accessed: 25 May 2023).

VANDEKERKHOVE, E., VAN DAELE, M., PRAET, N., CNUDDÉ, V., HAEUSSLER, P. J. & DE BATIST, M. 2020. Flood-triggered versus earthquake-triggered turbidites: A sedimentological study in clastic lake sediments (Eklutna Lake, Alaska). *Sedimentology*, 67, 364-389.

WHITE, B. J. P., SMITH, R. B., HUSEN, S., FARRELL, J. M. & WONG, I. 2009. Seismicity and earthquake hazard analysis of the Teton–Yellowstone region, Wyoming. *Journal of Volcanology and Geothermal Research*, 188, 277-296.

WIELAND, M. 2014. Seismic hazard and seismic design and safety aspects of large dam projects. *Perspectives on European Earthquake engineering and seismology*, 1, 627-650.

WILLIAMS, G. P. & WOLMAN, M. G. 1984. *Downstream effects of dams on alluvial rivers*, US Government Printing Office.

WURTSBAUGH, W. 2014. Jackson Lake Limnology.

YEAGER, K. M., SANTSCHI, P. H. & ROWE, G. T. 2004. Sediment accumulation and radionuclide inventories ($^{239,240}\text{Pu}$, ^{210}Pb and ^{234}Th) in the northern Gulf of Mexico, as influenced by organic matter and macrofaunal density. *Marine Chemistry*, 91, 1-14.

YEH, S.-W., KUG, J.-S., DEWITTE, B., KWON, M.-H., KIRTMAN, B. P. & JIN, F.-F. 2009. El Niño in a changing climate. *Nature*, 461, 511-514.

ZAREMBA, N. AND SCHOLZ, C.A. 2021. Evidence for ice-calving at the terminus of a Laurentide ice stream from multichannel seismic reflection data, Oneida Lake, NY. *Quaternary research*.

ZELLMAN, M., DUROSS, C. B., THACKRAY, G. D., BRIGGS, R. W., CHOLEWINSKI, N., REYES, T., PATTON, N. & MAHAN, S. A. 2018. A Paleoseismic investigation of the northern Teton fault at the Steamboat Mountain trench site, Grand Teton National Park, Wyoming. *Seismological Research Letters*, 89, 837.

ZELLMAN, M. S., DUROSS, C. B., THACKRAY, G. D., PERSONIUS, S. F., REITMAN, N. G., MAHAN, S. A. & BROSSY, C. C. 2020. Holocene Rupture History of the Central Teton Fault at Leigh Lake, Grand Teton National Park, Wyoming. *Bulletin of the Seismological Society of America*, 110, 67-82

VITA

1. Place of birth: Greencastle, Indiana
2. Educational institutions attended and degrees already awarded: B.S. in Geology awarded from Indiana State University
3. Professional positions held: Graduate Research Assistant, Graduate Teaching Assistant, Student Director of John C. Hook Observatory, Freshwater Stream Hydrology Research Assistant, and Student Researcher
4. Scholastic and professional honors: Summa Cum Laude for bachelor's degree
5. Professional publications:
 - Alverson, A. J., Chafin, T. K., Jones, K. A., Manoylov, K. M., **Johnson, H.**, Julius, M. L., ... & Stone, J. R. (2021). Microbial biogeography through the lens of exotic species: the recent introduction and spread of the freshwater diatom *Discostella asterocostata* in the United States. *Biological Invasions*, 23, 2191-2204.
 - McGlue, M. M., Dilworth, J. R., **Johnson, H. L.**, Whitehead, S. J., Thigpen, J. R., Yeager, K. M., ... & Swanger, W. R. (2023). Effect of Dam Emplacement and Water Level Changes on Sublacustrine Geomorphology and Recent Sedimentation in Jackson Lake, Grand Teton National Park (Wyoming, United States). *Earth Science, Systems and Society*, 2.
6. Hillary L. Johnson